Combined Analysis: structure, microstructure, texture, stresses, phase, reflectivity

Daniel Chateigner
IUT-Univ. Caen Basse-Normandie
CRISMAT-ENSICAEN (Caen-France)

1st INEL Workshop on Combined Analysis, Caen, 28th june – 2nd July 2010

Structure determination on real (textured) samples
Dilemma 1

Structure and QTA: correlations: f(g) and $|F_{\mathbf{h}}|^2$ are different !

f(g):

-Angularly constrained: $[h_1k_1l_1]^*$ and $[h_2k_2l_2]^*$ make a given angle: more determined if F^2 high

- lot of data (spectra) needed

$|F_{\mathbf{h}}|^2$:

-Position, f_i, and Debye-Waller constrained

- work on the sum of all diagrams on average

Texture from Spectra

Orientation Distribution Function (ODF)

From pole figures

From spectra

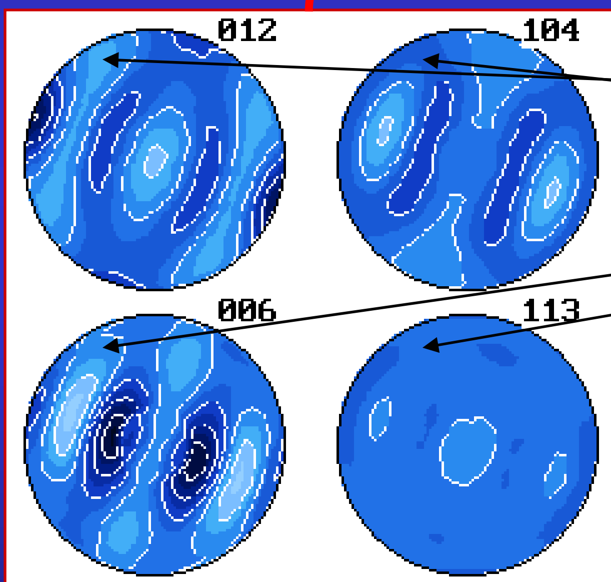

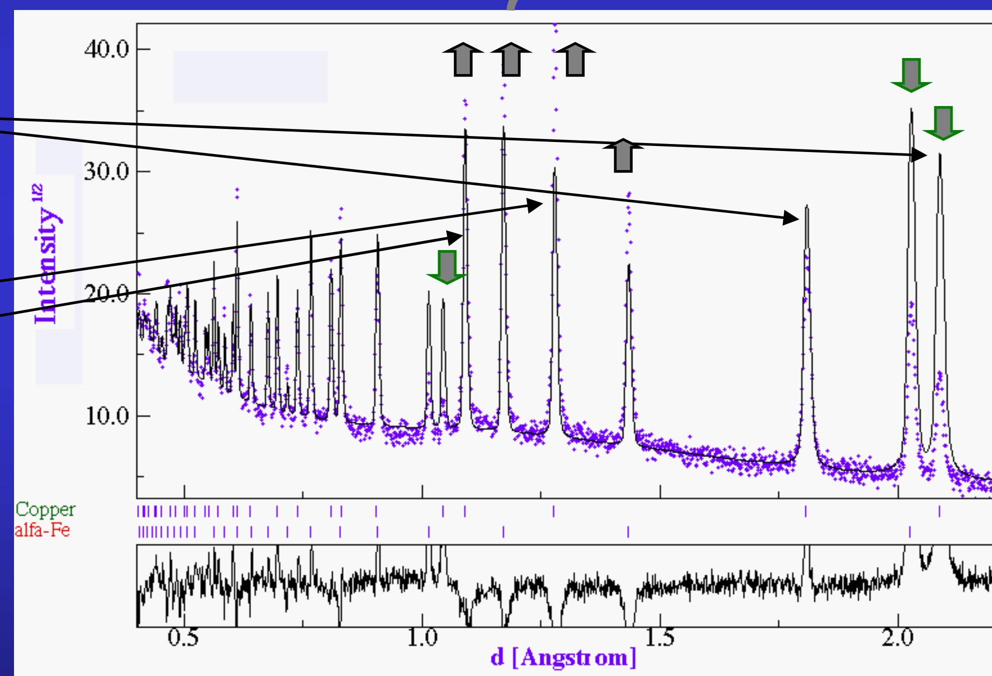

Le Bail extraction + ODF: WMV, E-WIMV, Generalized spherical harmonics, components, ADC, entropy maximisation …

Why not benefit of texture in Structure determination ?

Perfect powders:
- overlaps (intra- and inter-p
- no angular constrain
- anisotropy difficult to resc

Single pattern

Single crystals:
- reduced overlaps
- max angular constrains
- Perfect texture: max anisotropy

Many individual diffracted peaks

Textured powders:
- reduced overlaps
- angular constrain = f(texture strength)
- Intermediate anisotropy

Many patterns to measure and analyse

Rietveld-Structure

$$I_i^{calc}(\chi,\phi) = \sum_{n=1}^{Nphases} S_n \sum_k L_k \left|F_{k;n}\right|^2 S\left(2\theta_i - 2\theta_{k;n}\right) P_{k;n}(\chi,\phi) A + bkg_i$$

Texture

$$P_k(\chi,\phi) = \int_{\varphi} f(g,\varphi)\, d\varphi$$

- Generalized Spherical Harmonics (Bunge):

$$P_k(\chi,\phi) = \sum_{l=0}^{\infty} \frac{1}{2l+1} \sum_{n=-l}^{l} k_l^n(\chi,\phi) \sum_{m=-l}^{l} C_l^{mn} k_n^{*m}\left(\Theta_k \phi_k\right)$$

$$f(g) = \sum_{l=0}^{\infty} \sum_{m,n=-l}^{l} C_l^{mn} T_l^{mn}(g)$$

- Components (Helming):

$$f(g) = F + \sum_c I^c f^c(g)$$

- WIMV (William, Imhof, Matthies, Vinel) iterative process:

$$f^{n+1}(g) = N_n \frac{f^n(g) f^0(g)}{\left(\prod_{\mathbf{h}=1}^{I} \prod_{m=1}^{M_h} P_{\mathbf{h}}^n(\mathbf{y}) \right)^{\frac{1}{IM_h}}}$$

$$f^0(g) = N_0 \left(\prod_{\mathbf{h}=1}^{I} \prod_{m=1}^{M_h} P_{\mathbf{h}}^{exp}(\mathbf{y}) \right)^{\frac{1}{IM_h}}$$

E-WIMV (Rietveld only):

$$f^{n+1}(g) = f^n(g) \prod_{m=1}^{M_h} \left(\frac{P_{\mathbf{h}}(\mathbf{y})}{P_{\mathbf{h}}^n(\mathbf{y})} \right)^{r_n \frac{w_h}{M_h}}$$

with $0 < r_n < 1$, relaxation parameter,
M_h number of division points of the integral around k,
w_h reflection weight

- Entropy maximisation (Schaeben):

$$f^{n+1}(g) = f^n(g) \prod_{m=1}^{M_h} \left(\frac{P_{\mathbf{h}}(\mathbf{y})}{P_{\mathbf{h}}^n(\mathbf{y})} \right)^{\frac{r_n}{M_h}}$$

- arbitrarily defined cells (ADC, Pawlik): Very similar to E-WIMV, with integrals along path tubes

Residual Stresses shift peaks with y

Dilemma 2

Stress and QTA: correlations: f(g) and C_{ijkl}

f(g):

- Moves the $\sin^2\Psi$ law away from linear relationship
- Needs the integrated peak (full spectra)

strains:

- Measured with pole figures
- needs the mean peak position

Isotropic samples: triaxial, biaxial, uniaxial stress states

Textured samples: Reuss, Voigt, Hill, Bulk geometric mean approaches

Residual Stresses and Rietveld

- **Macro elastic strain tensor (I kind)**
- **Crystal anisotropic strains (II kind)**

C

Macro and micro stresses

Applied macro stresses

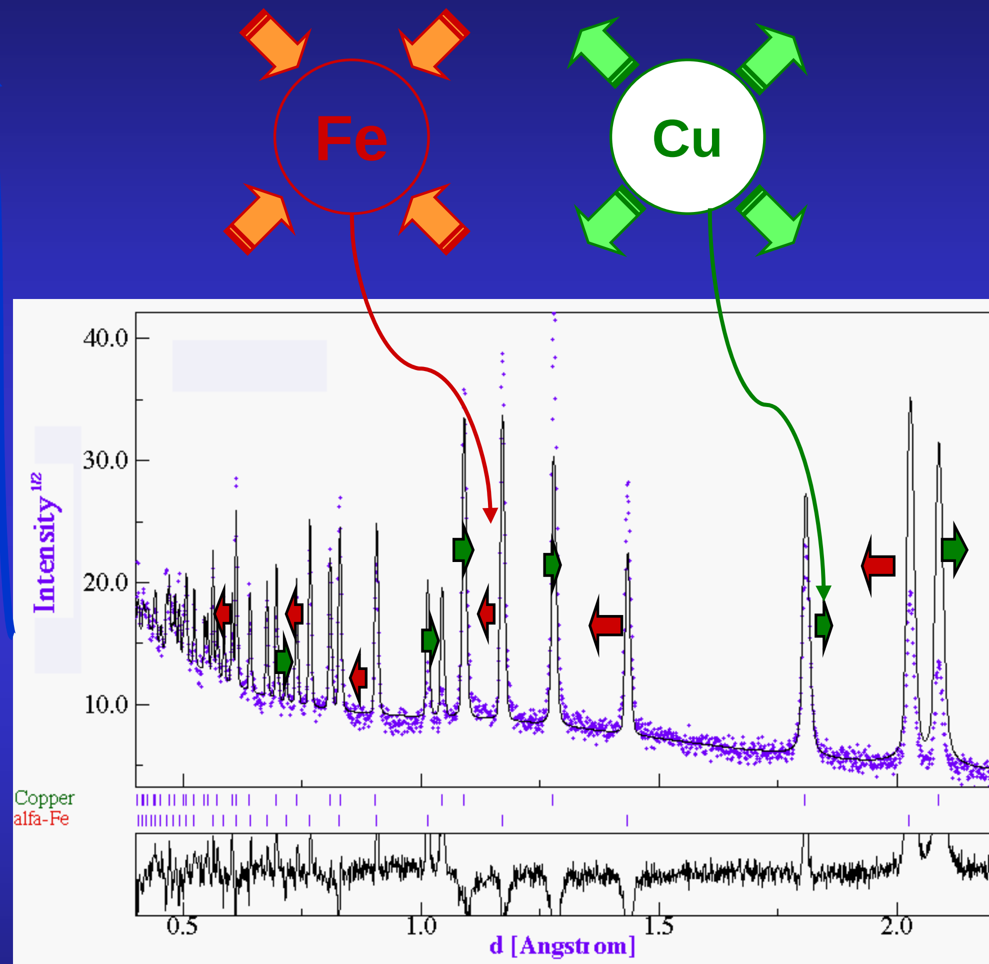

Isotropic samples: triaxial, biaxial, uniaxial stress states

Textured samples: Reuss, Voigt, Hill, Bulk geometric mean approaches

Strain-Stress

$$\boldsymbol{\varepsilon}(\mathbf{X}) = \boldsymbol{\varepsilon}^{\mathrm{I}} + \boldsymbol{\varepsilon}^{\mathrm{II}}(\mathbf{X}) + \boldsymbol{\varepsilon}^{\mathrm{III}}(\mathbf{X})$$

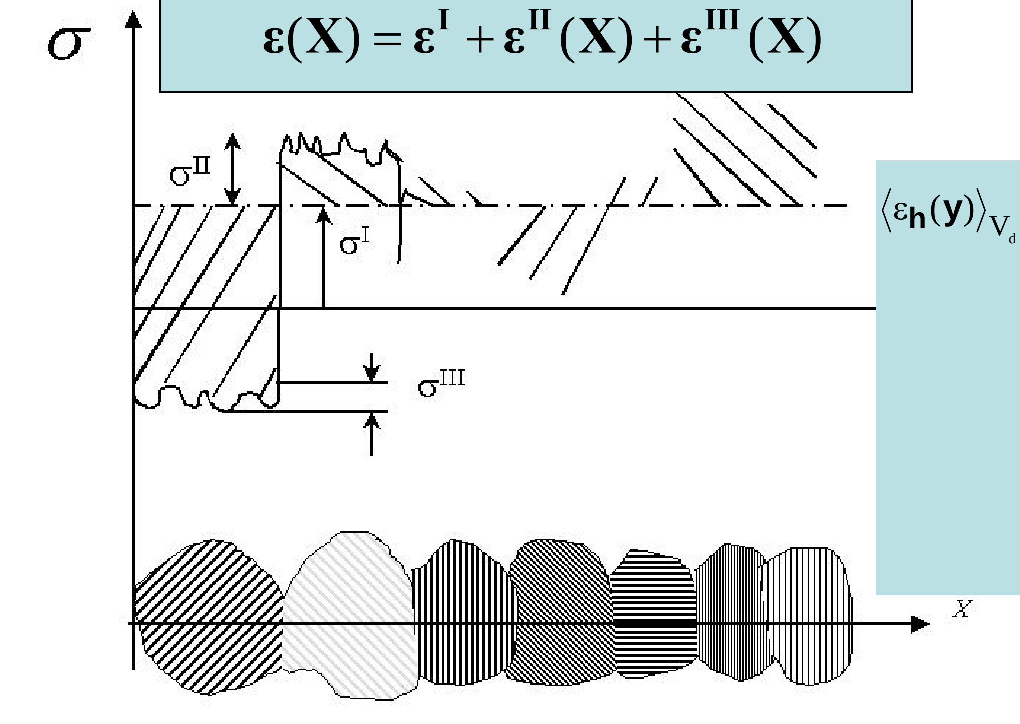

Isotropic samples:
triaxial, biaxial uniaxial stress state

$$\langle \varepsilon_{\mathbf{h}}(\mathbf{y}) \rangle_{V_d} = \frac{1}{V_d} \int_{V_d} (\varepsilon_{33}^{I} + \varepsilon_{33}^{II} + \varepsilon_{33}^{III}) dV$$

$$= (\varepsilon_{11}^{I} \cos^2\phi + \varepsilon_{12}^{I} \sin 2\phi + \varepsilon_{22}^{I} \sin^2\phi - \varepsilon_{33}^{I}) \sin^2\psi + \varepsilon_{33}^{I} +$$

$$(\varepsilon_{13}^{I} \cos\phi + \varepsilon_{23}^{I} \sin\phi) \sin 2\psi + \frac{1}{V_d} \int_{V_d} (\varepsilon_{33}^{IIe} + \varepsilon_{33}^{IIti} + \varepsilon_{33}^{IIpi}) dV$$

$$= \frac{\langle d(hkl, \phi, \psi) \rangle_{V_d} - d_0(hkl)}{d_0(hkl)}$$

Textured samples:
triaxial, biaxial uniaxial stress state
+ ODF + SDF + model

$$\langle E(\mathbf{g}) \rangle_{V_d} = \frac{1}{V_d} \int_{V_d} E^{SC}(g) f(g) dg$$

$$= \left(\prod_{V_d} E^{SC}(g) f(g) dg \right)^{\frac{1}{V_d}}$$

$$\chi^2 = \sum_i w_i^2 \left[\varepsilon_i^{calc}(S_{ijk\ell}^{M}, \mathbf{h}, \mathbf{y}) - \varepsilon_i^{meas}(S_{ijk\ell}^{M}, \mathbf{h}, \mathbf{y}) \right]^2$$

Non-linear least-square fit

Layered systems

Dilemma 3

Layer, Rietveld and QTA: correlations: f(g), thicknesses and structure

f(g):

- Pole figures need corrections for abs-vol
- Rietveld also to correct intensities

layers:

- unknown sample true absorption coefficient μ
- unknown effective thickness (porosity)

Layering

Asymmetric Bragg-Brentano

$$C_\chi^{\text{top film}} = g_1\left(1-\exp\left(-\mu T g_2/\cos\chi\right)\right)/\left(1-\exp\left(-2\mu T/\sin\omega\cos\chi\right)\right)$$

$$C_\chi^{\text{cov. layer}} = C_\chi^{\text{top film}}\left(\exp\left(-g_2\sum\mu_i^{'}T_i^{'}/\cos\chi\right)\right)/\left(\exp\left(-2\sum\mu_i^{'}T_i^{'}/\sin\omega\cos\chi\right)\right)$$

Probes μT

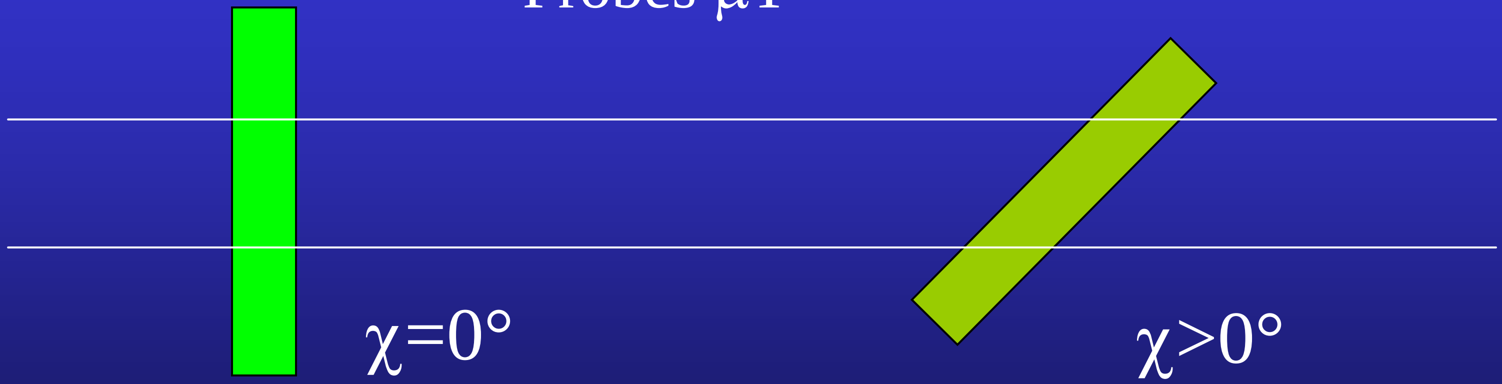

Phase and Texture

Dilemma 4

Phase and QTA: correlations: f(g), S_Φ

f(g):

- angular relationships
- plays on individual spectra
- essential to operate on textured sample

S_Φ:

- plays on overall scale factor (sum diagram)

Phase analysis

- Volume fraction

$$V_{\Phi} = \frac{S_{\Phi} V_{uc\Phi}^{2}}{\sum_{\Phi} \left(S_{\Phi} V_{uc\Phi}^{2} \right)_{\Phi}}$$

- Weight fraction

$$m_{\Phi} = \frac{S_{\Phi} Z_{\Phi} M_{\Phi} V_{uc\Phi}^{2}}{\sum_{\Phi} \left(S_{\Phi} Z_{\Phi} M_{\Phi} V_{uc\Phi}^{2} \right)_{\Phi}}$$

Z = number of formula units

M = mass of the formula unit

V = cell volume

How it works

Le Bail extraction

$$T_{hkl}^{k} = T_{hkl}^{k-1} \frac{\sum_{i} I_i^{exp} S_{hkl}^{i}}{\sum_{i} I_i^{calc} S_{hkl}^{i}}$$

- Starts with nominal intensities (T_{hkl})
- Computes the full pattern (I^{calc})
- Uses the formula to compute next T_{hkl}
- Cycle the last two steps until convergence

- In Maud, options:
  - Only few cycles for texture (3-5) necessary
  - The range for the weighting of the profile can be reduced
  - Background subtracted or not

Structure and Residual Stresses (shift peaks with **y**)
Dilemma 5

Stress and cell parameters: correlations: peak positions and C_{ijkl}

Cell parameters:
- Measured at high angles
- Bragg law evolution

strains:
- Measured precisely at high angles
- stiffness-based variation, also with Ψ

Shapes, microstrains, defaults, distributions
Dilemma 6

Shapes …. and stress-texture-structure: correlations ?

Shapes …:

- line broadening problem
- average positions modified
- if anisotropic: modification changes with **y**

Stress-texture-structure:

- need "true" peak positions and intensities
- need deconvoluted signals

Scherrer, Integral breadth, Williamson-Hall …

$$\langle D\rangle_v = \frac{K\lambda}{\beta_S(2\theta)\ \cos\theta}$$

More elegant, mandatory for whole-pattern: Stokes deconvolution
Bertaut-Warren-Averbach treatment, e.g. for a 00l peak:

$$A_n = A_n^S A_n^D = \frac{N_n}{N_3}\langle \cos 2\pi l Z_n \rangle$$

$$A_n^S = \frac{N_n}{N_3} = \frac{1}{N_3}\sum_{i=|n|}^{\inf}(i-|n|)\,p(i)$$

$$\left(\frac{dA_n^S}{dn}\right)_{n\to 0} = -\frac{1}{N_3}$$

Second derivative: distribution of column lengths

Anisotropic sizes and microstrains

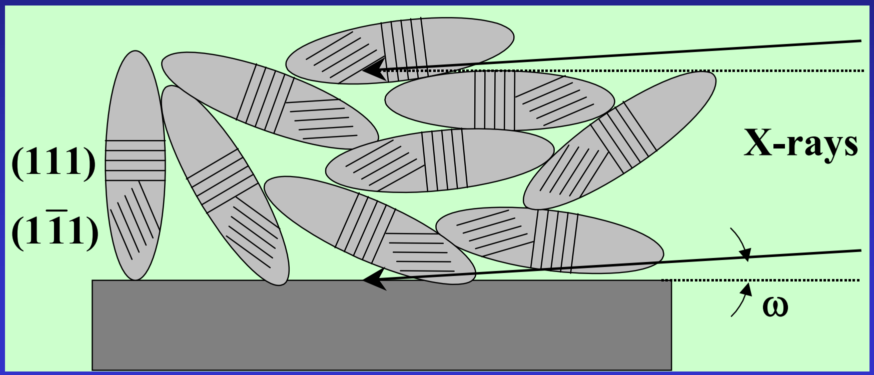

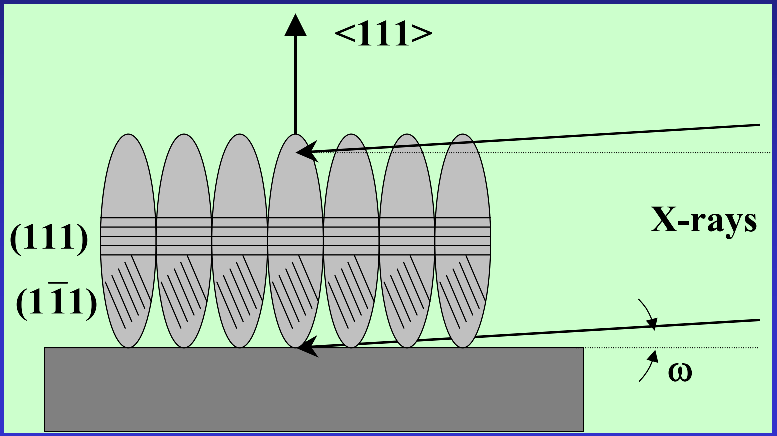

- Texture helps the "real" mean shape determination
- Determination by peak deconvolution + Popa formalism

$$\langle R_{\mathbf{h}} \rangle = R_0 + R_1 P_2^{0}(x) + R_2 P_2^{1}(x)\cos\varphi + R_3 P_2^{1}(x)\sin\varphi + R_4 P_2^{2}(x)\cos 2\varphi + R_5 P_2^{2}(x)\sin 2\varphi + \ldots$$

$$\langle \varepsilon_{\mathbf{h}}^{2} \rangle E_{\mathbf{h}}^{4} = E_1 h^4 + E_2 k^4 + E_3 \ell^4 + 2E_4 h^2 k^2 + 2E_5 \ell^2 k^2 + 2E_6 h^2 \ell^2 + 4E_7 h^3 k + 4E_8 h^3 \ell + 4E_9 k^3 h + 4E_{10} k^3 \ell + 4E_{11} \ell^3 h + 4E_{12} \ell^3 k + 4E_{13} h^2 k \ell + 4E_{14} k^2 h \ell + 4E_{15} \ell^2 k h$$

Combined Analysis approach

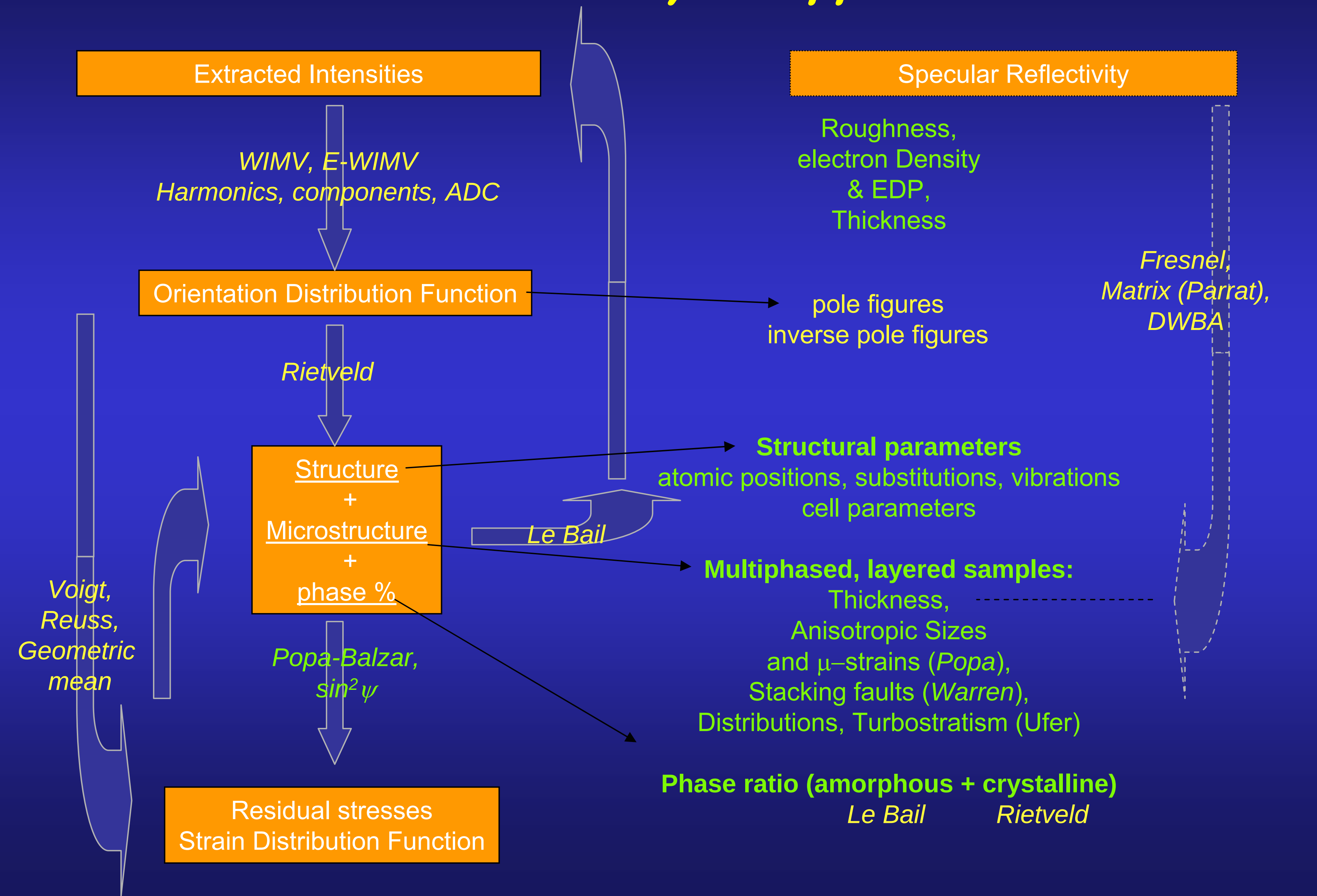

Grinding to powderise another dilemma !

Grinding: removes angular relationship, adds correlations

Texture:

- not measured
- removed ? hope to get a perfect powder

Strains, defaults, anisotropy … :

- some removed, some added

Same sample ?

Rare samples ?

Minimum experimental requirements

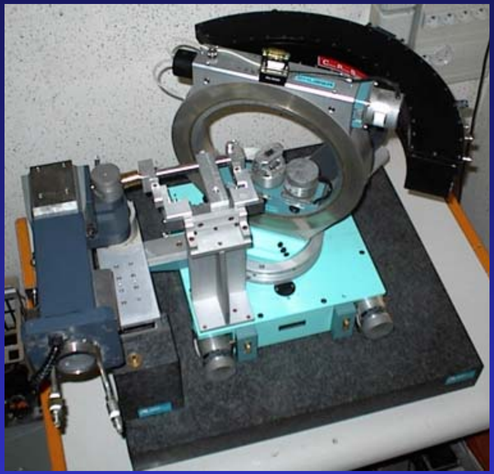

1D or 2D Detector + 4-circle diffractometer
(X-rays and neutrons)
CRISMAT, ILL

+

~1000 experiments (2θ diagrams)
in as many sample orientations

+

Instrument calibration
(peaks widths and shapes,
misalignments, defocusing …)

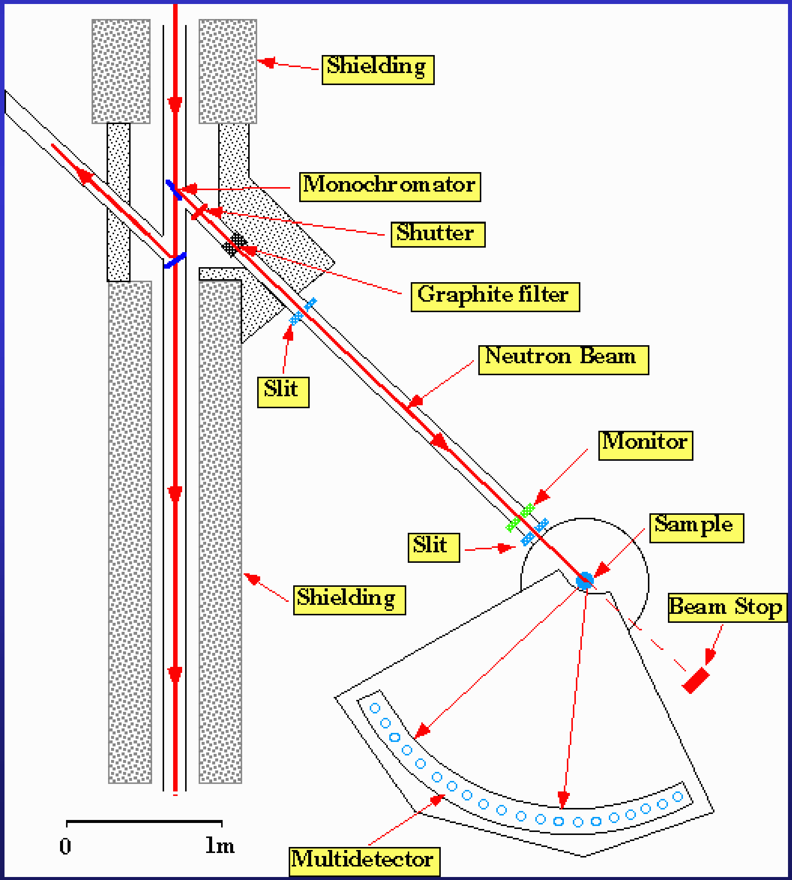

2D Curved Area Position Sensitive Detector

D19 - ILL

+

~100 experiments (2D Debye-Scherrer diagrams)
in as many sample orientations

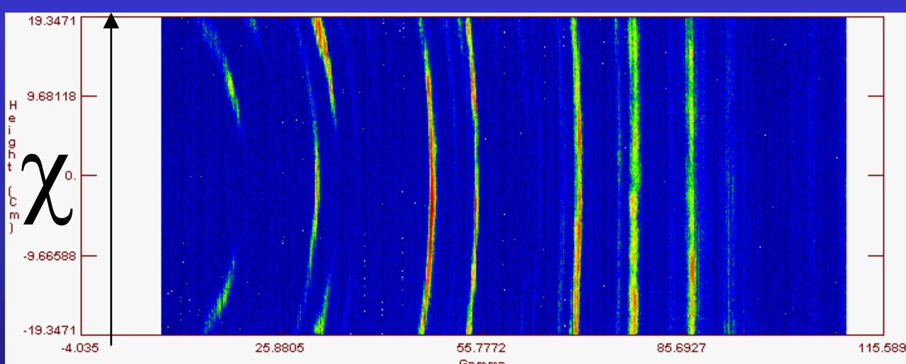

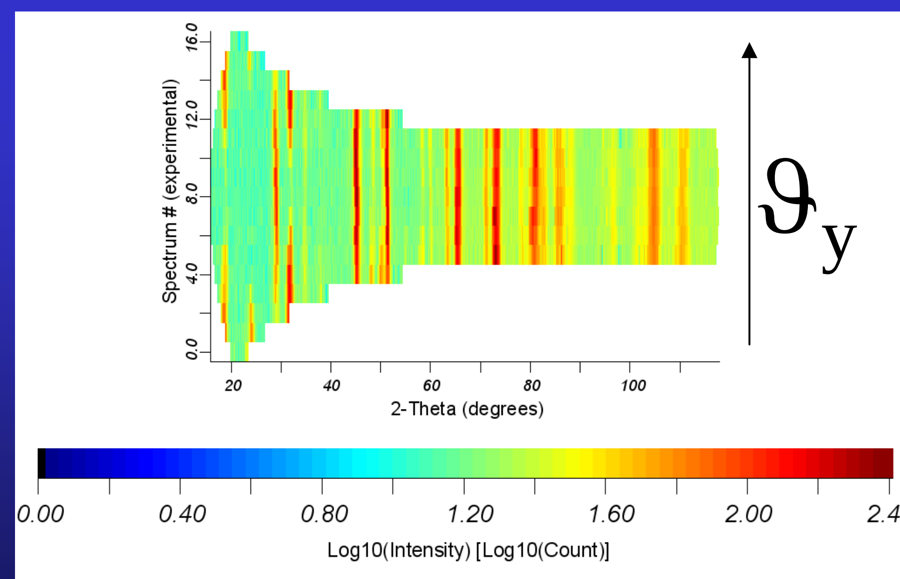

Calibration

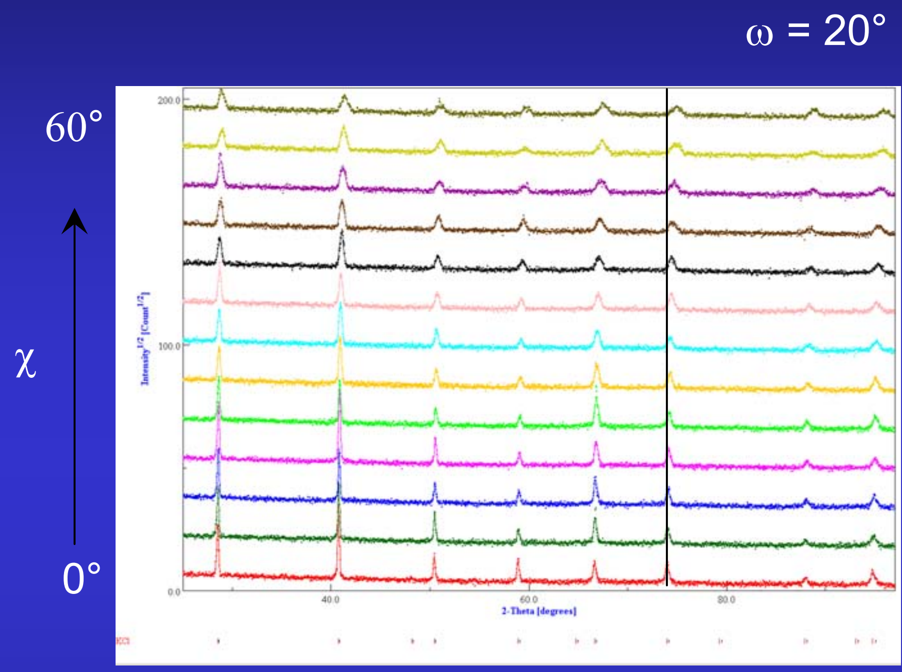

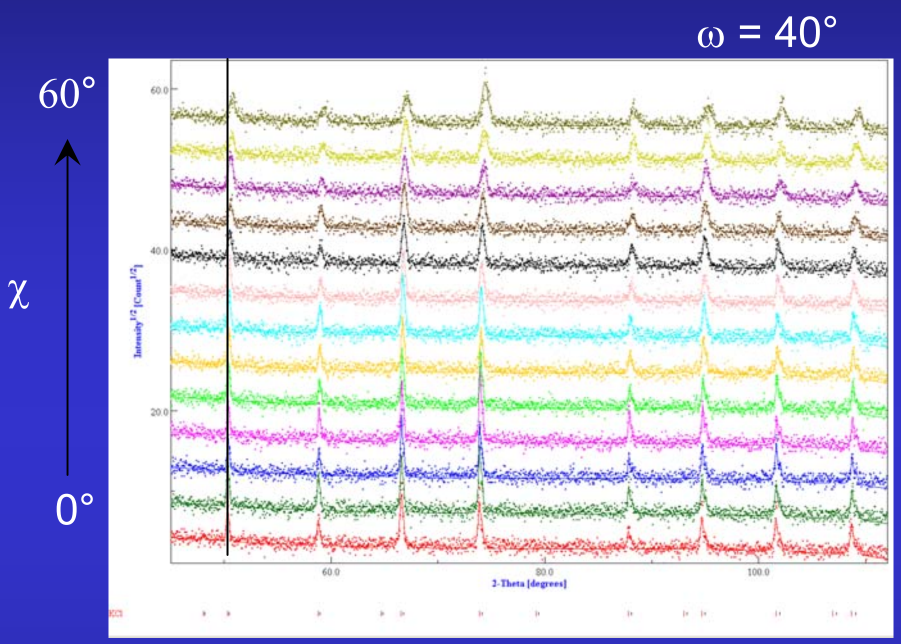

KCl, LaB_6 …

FWHM (ω, χ, 2θ …)
2θ shift
gaussianity
asymmetry
misalignments ...

Minimization algorithms

- Can be fully used in the method (everywhere)

- Marquardt Least Squares (based on steepest decrease and Gauss-Newton)
  - Efficient, best with few parameters, near the solution
- Evolutionary computation (or genetic algorithm)
  - Slow, not efficient, requires a lot of resources
  - Unlimited number of parameters
  - Can start far from the solution
- Simulated annealing (the solution proceed like a random walk, but the walking step decreases as temperature decreases)
  - In between the Marquardt and evolutionary algorithms
- Simplex (generates n+1 starting solutions as vertices of a polygon, n number of parameters, and contract/expand the polygon around the minima)
  - Slow on convergence
  - Remains close to the solution, but explore more minima with respect to the Marquardt

$Ca_3Co_4O_9$ thermoelectrics

$Ca_3Co_4O_9$: Misfit lamellar and modulated Structure, with high thermopower

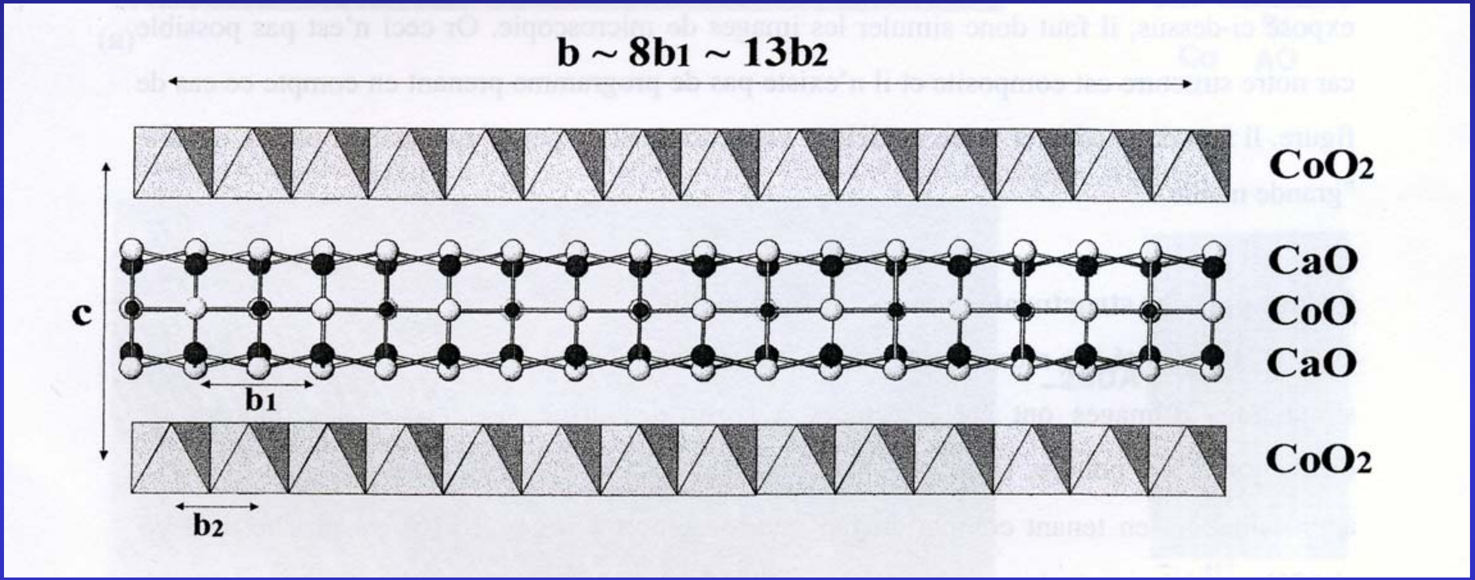

Two monoclinic sub-systems:
S1 with a ~ 4.8Å, b_1 ~ 4.5Å, c ~ 10.8Å et β ~ 98° (NaCl-type)
S2 with a ~ 4.8Å, b_2 ~ 2.8Å, c ~ 10.8Å et β ~ 98° (CdI_2-type)

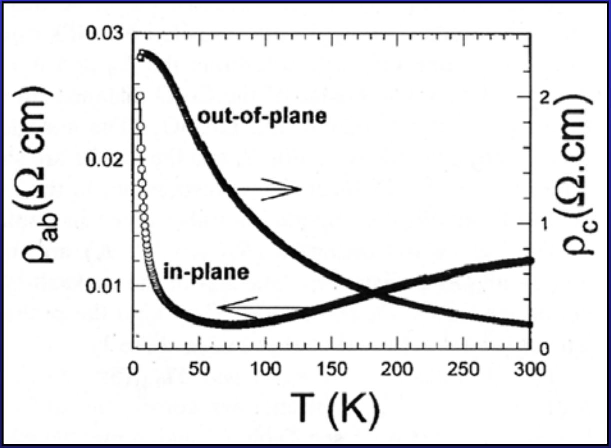

$\Gamma = \sigma_{ab}/\sigma_c \sim 10$ → Texture

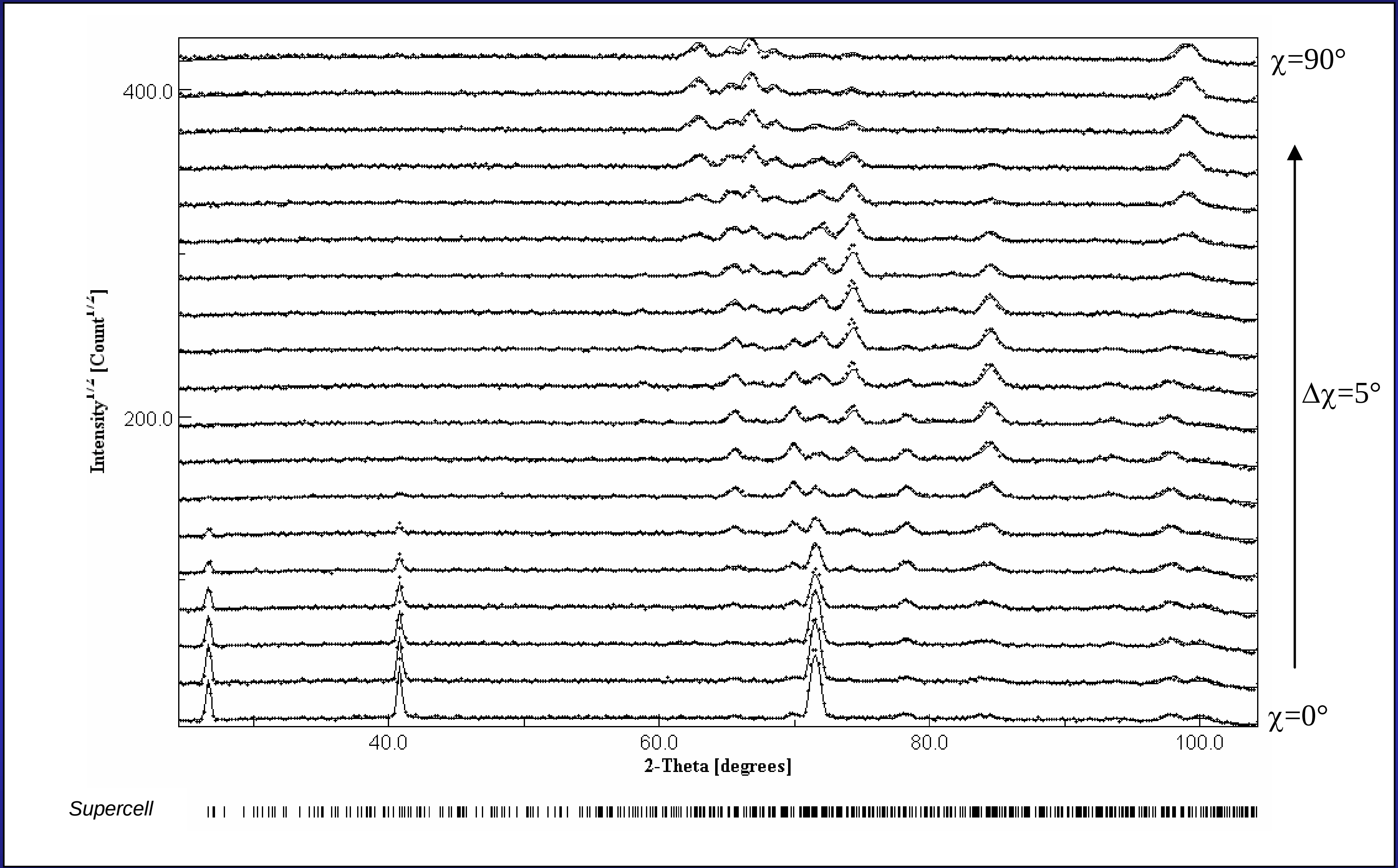

400.0
200.0
Intensity^1/2 [Count^1/2]
40.0
60.0
80.0
100.0
2-Theta [degrees]
χ=90°
Δχ=5°
χ=0°
Supercell

RP=19.7%, Rw=11.9%

9.8 MPa for 2 h

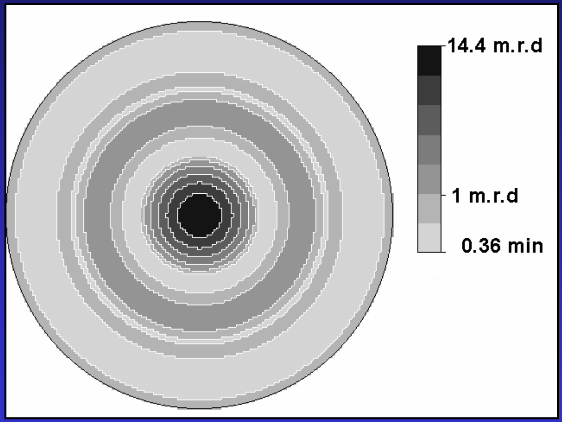

19.6 MPa for 6 h

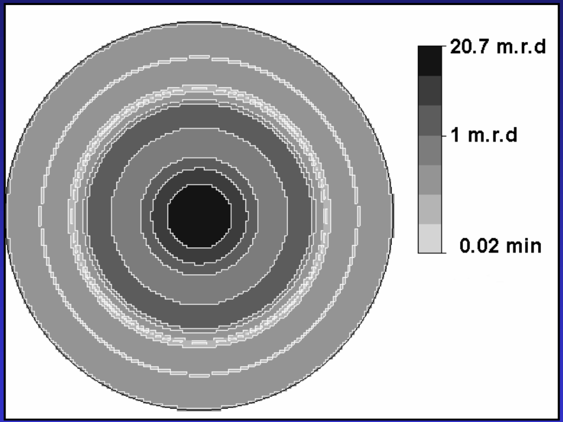

19.6 MPa for 20 h

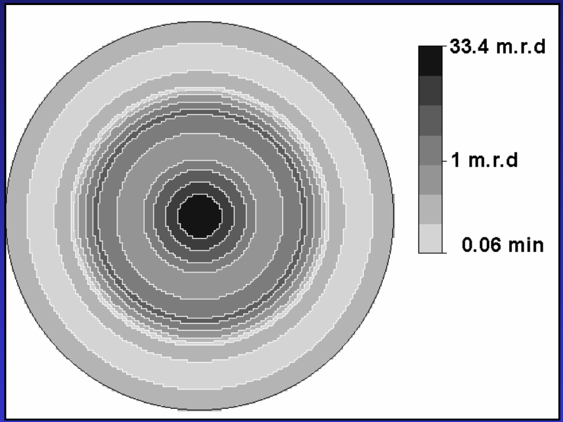

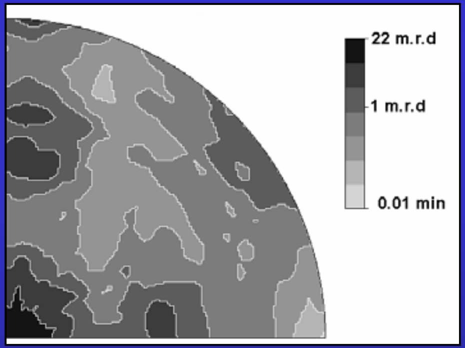

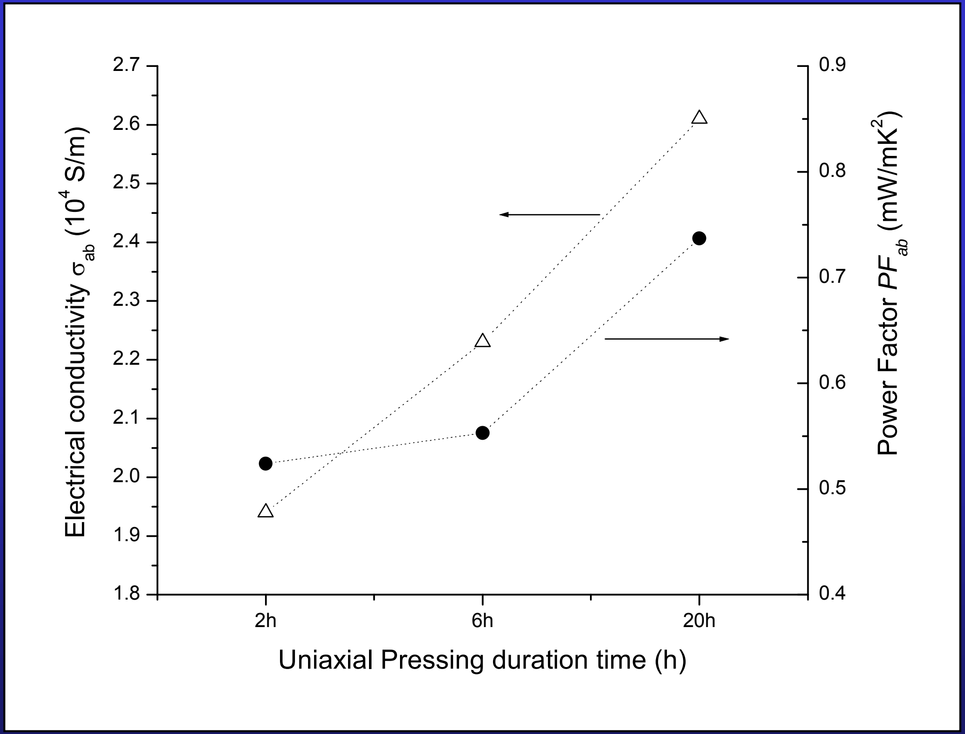

Templated Growth Method

Bi2223 compounds

E. Guilmeau, PhD

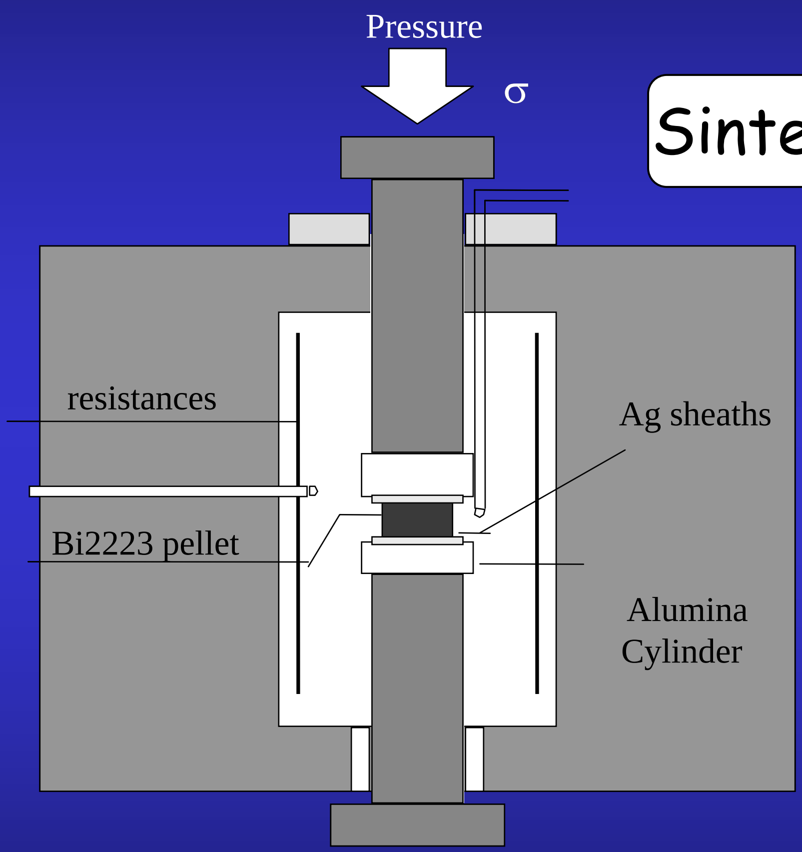

Sinter-Forging

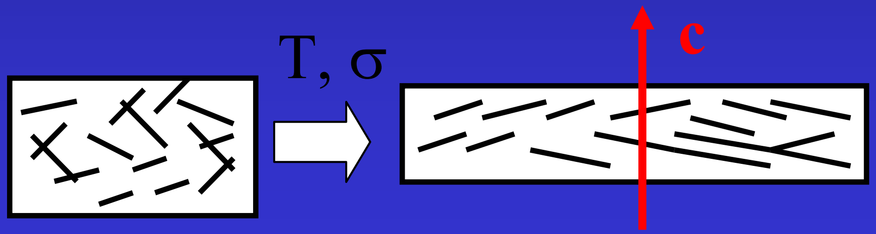

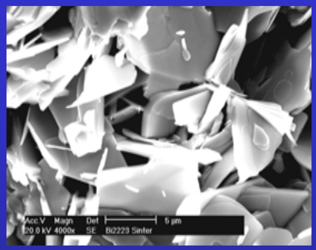

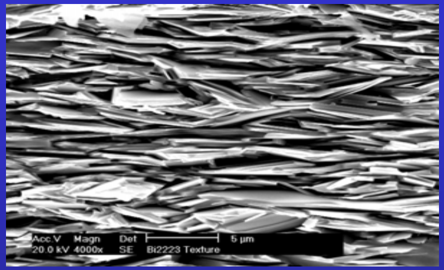

Grain alignment ⇒ $\nearrow$Jc

(00ℓ) Texture

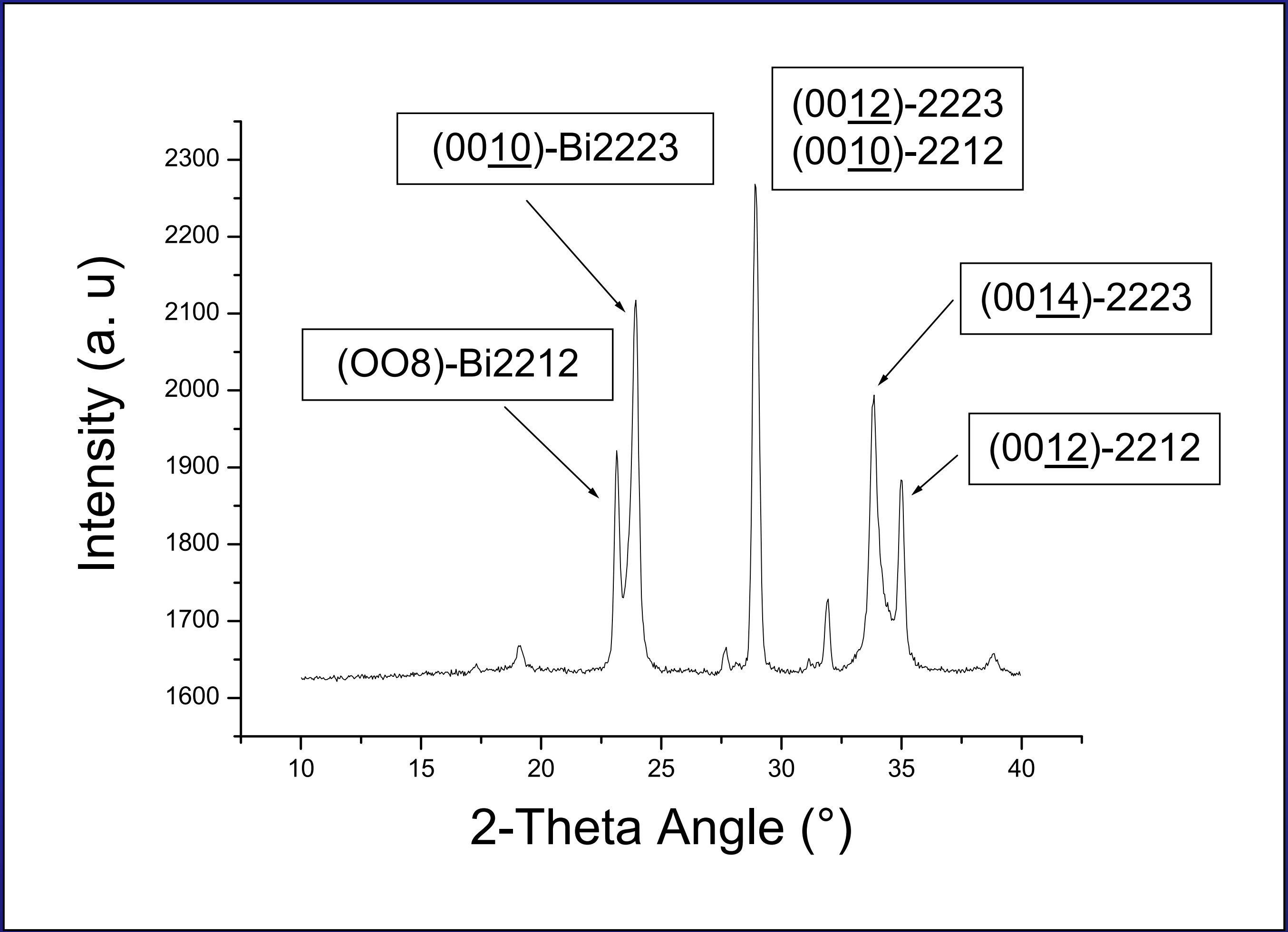
(0010)-Bi2223
(0012)-2223
(0010)-2212
(0014)-2223
(OO8)-Bi2212
(0012)-2212
Intensity (a. u)
2300
2200
2100
2000
1900
1800
1700
1600
10
15
20
25
30
35
40
2-Theta Angle (°)

Bi2212 + Secondary phases → Bi2223

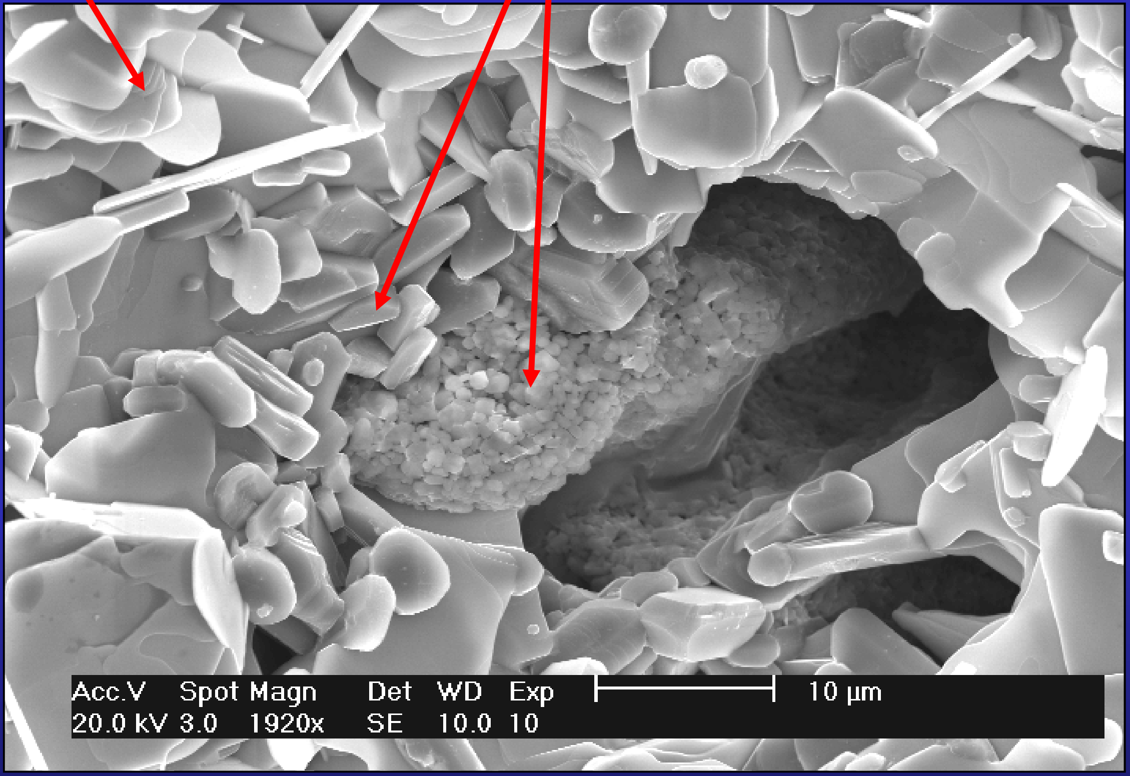

Combined Analysis

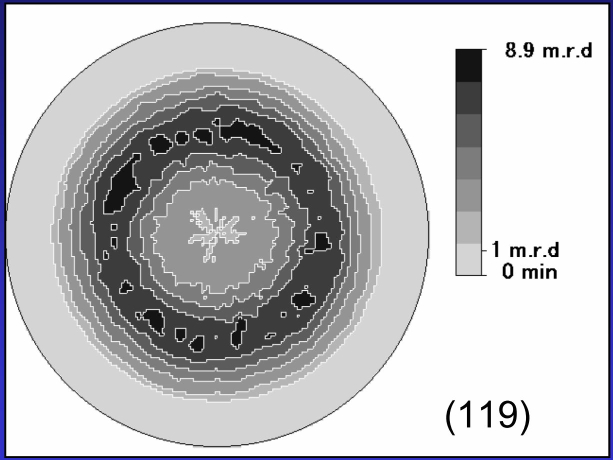

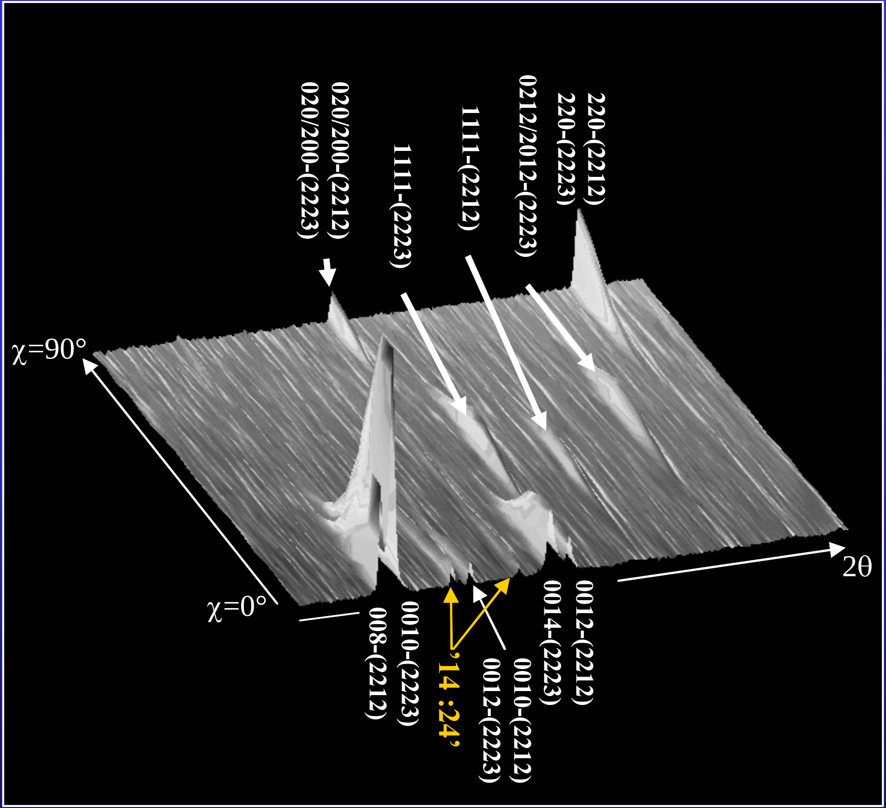

- *Neutrons*
- Sample: ~70 mm^3
- 2θ patterns for $\chi=0°$ to 90°
- No φ rotation (fibre texture).

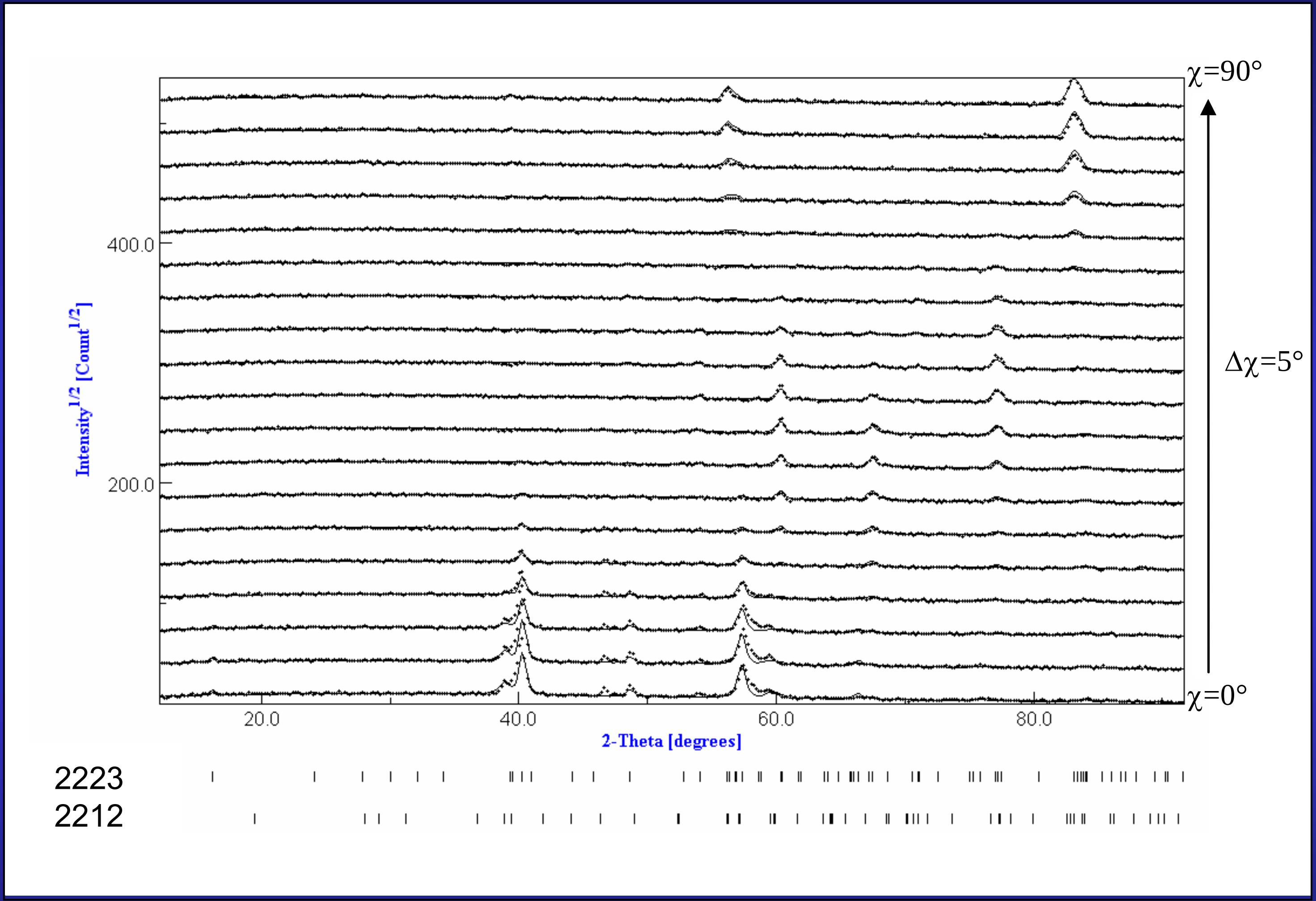

Rw=9.12

RP=16.24

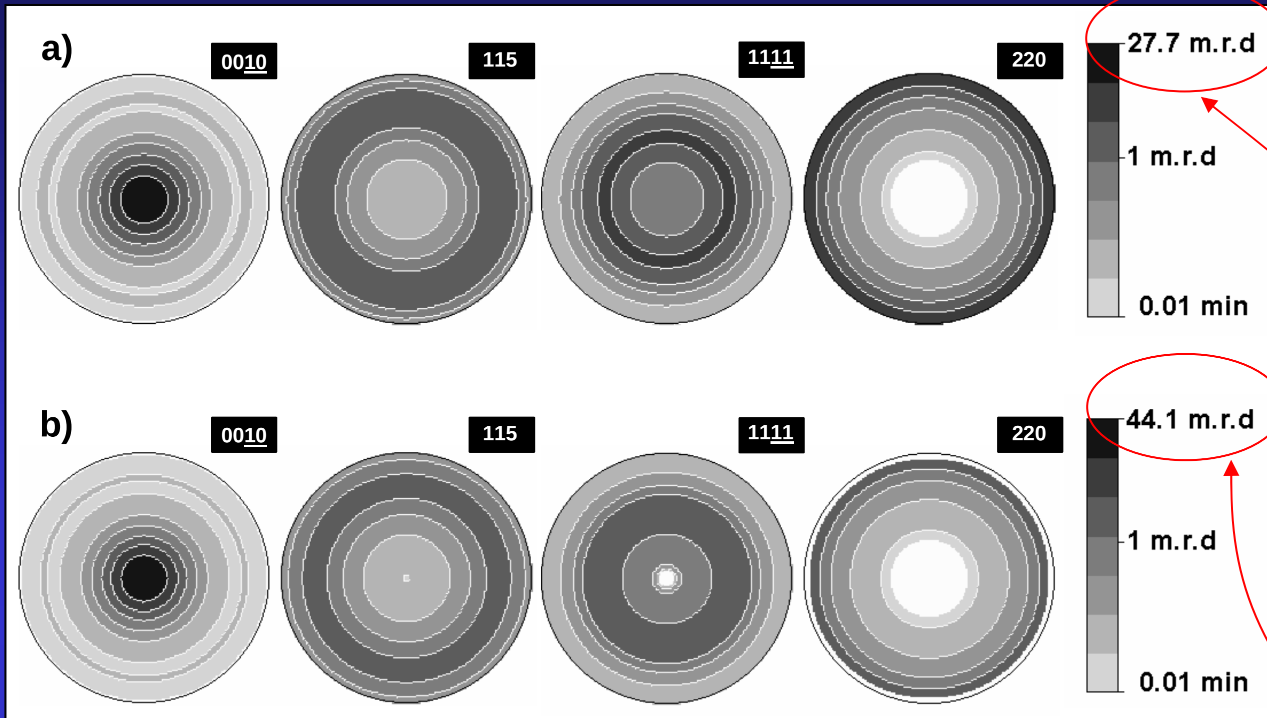

Logarithmic density scale, equal area projection

Recalculated (WIMV)

Extracted (Le Bail)

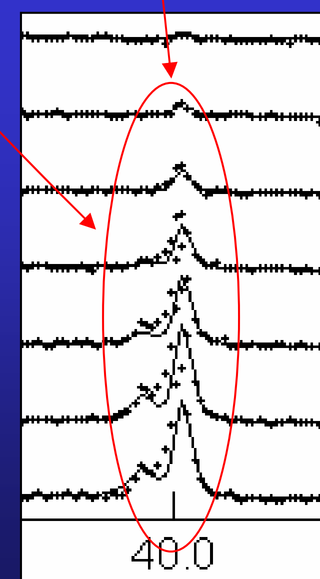

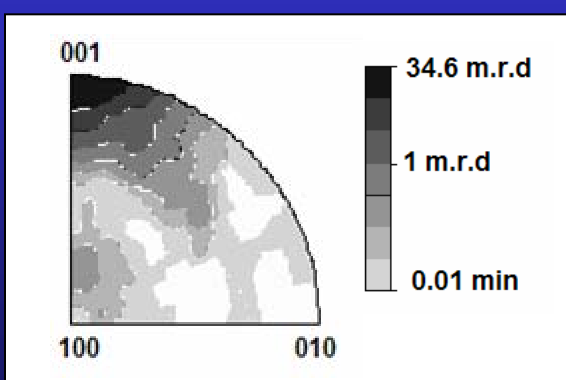

Logarithmic density scale, equal area projection

Stacking faults and/or intergrowth on the c-axis →New periodicities and peaks characterized with intermediate c parameters.

However, no algorithm is included to solve intergrowths in the combined approach.

Effect of the sinter-forging treatment on the texture development, crystal growth, transport properties

Sinter-forging dwell time (h)	*Orientation Distribution Max (m.r.d.)*		*% Bi2223*	*Cell parameters (Å)*		*Crystallite size Bi2223 (nm)*	*Rb (%)*	*Rw (%)*	*Rexp (%)*	*RP0 (%)*	*RP1 (%)*	*J_c (A/cm^2)*
	Bi2212	*Bi2223*		*Bi2223*	*Bi2212*							
20	21.8	20.7	59.9±1.3	a=5.419(3) b=5.391(3) c=37.168(3)	a=5.414(3) b=5.393(3) c=30.800(3)	205±7	7.56	11.1	4.55	17.74	10.56	12500
50	24.1	24.4	72.9±2.9	a=5.419(3) b=5.408(3) c=37.192(3)	a=5.416(3) b=5.396(3) c=30.806(3)	273±10	7.54	11.37	4.58	17.05	11.04	15000
100	31.5	25.2	84.4±4.6	a=5.410(3) b=5.405(3) c=37.144(3)	a=5.412(3) b=5.403(3) c=30.752(3)	303±10	5.4	8.04	3.69	13.54	9.31	19000
150	65.4	27.2	87.0±4.1	a=5.417(3) b=5.403(3) c=37.199(3)	a=5.413(3) b=5.407(3) c=30.792(3)	383±13	6.13	9.12	4.8	16.24	12.25	20000

↗ Texture strength

↗ *Sinter-forging Time* ⇒ ↗ % Bi2223 ⇔ ↗ J_c

↗ Crystallite Size

E. Guilmeau et al., JAC

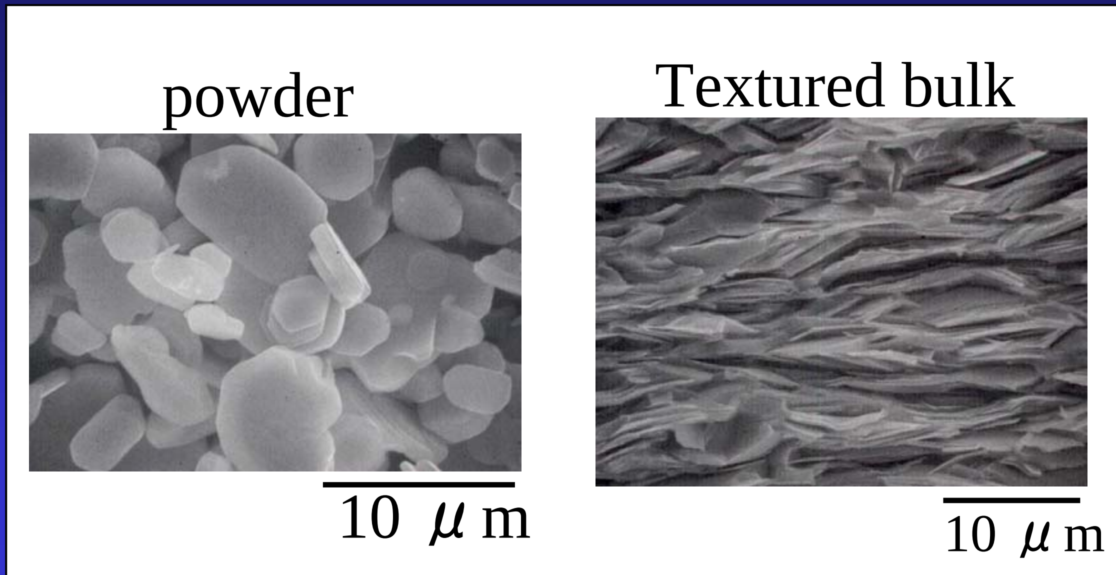

Magnetic alignment
and
Templated Growth
method

Analysis:

- *neutrons*
- *3D Supercell: a=4.8309Å, b~8b1~13b2~36.4902Å, c=10.8353Å, β=98.13°*
174 atoms/cell
-Sample : 0.6 cm^3

Magnetic Alignment

Logarithmic density scale, equal area projection

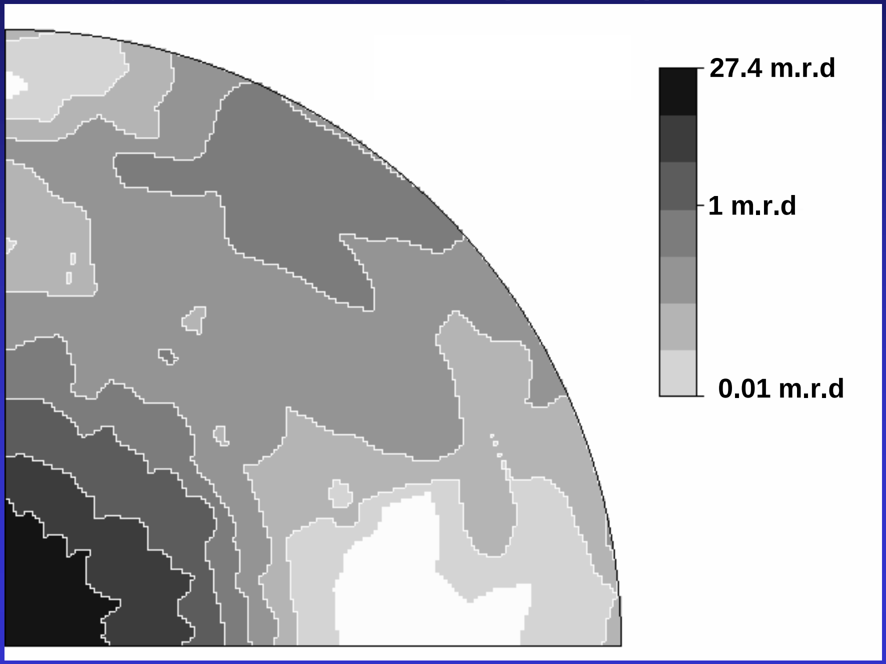

- magnetic alignment really efficient to obtain strong textures

- combined analysis of modulated structures possible

Ferroelectric PCT films

J. Ricote, Madrid

thin films:

$(Ca_{0.24}Pb_{0.76})TiO_3$ sol-gel synthesised solutions deposited by spin coating on a substrate of $Pt/TiO_2/Si$, with and without a treatment at 650ºC for 30 min.

All films are crystallised at 700ºC for 50 s by Rapid Thermal Processing (RTP; 30ºC/s). A series is also recrystallised at 650ºC for 1 to 3 h.

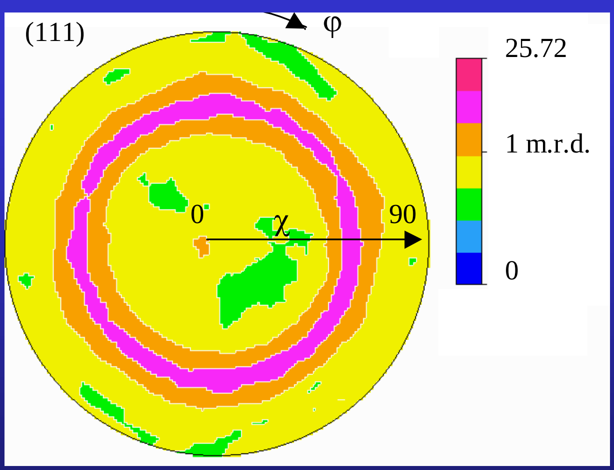

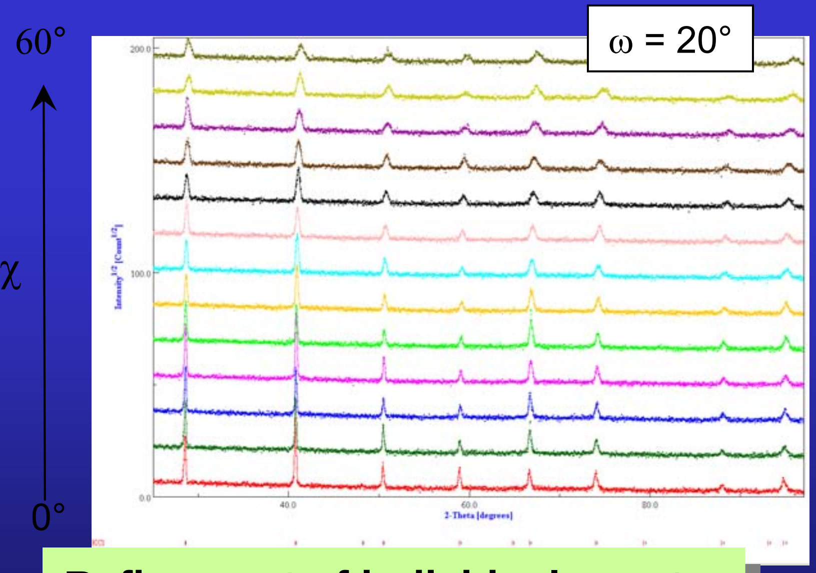

Refinement of individual spectra

Limitations of the simple Quantitative Texture Analysis

Structural parameters are difficult to obtain due to:

Substrate influence:
overlapping of reflections from the film and the substrate

TEXTURE effects:
peaks that do not appear at low χ angles

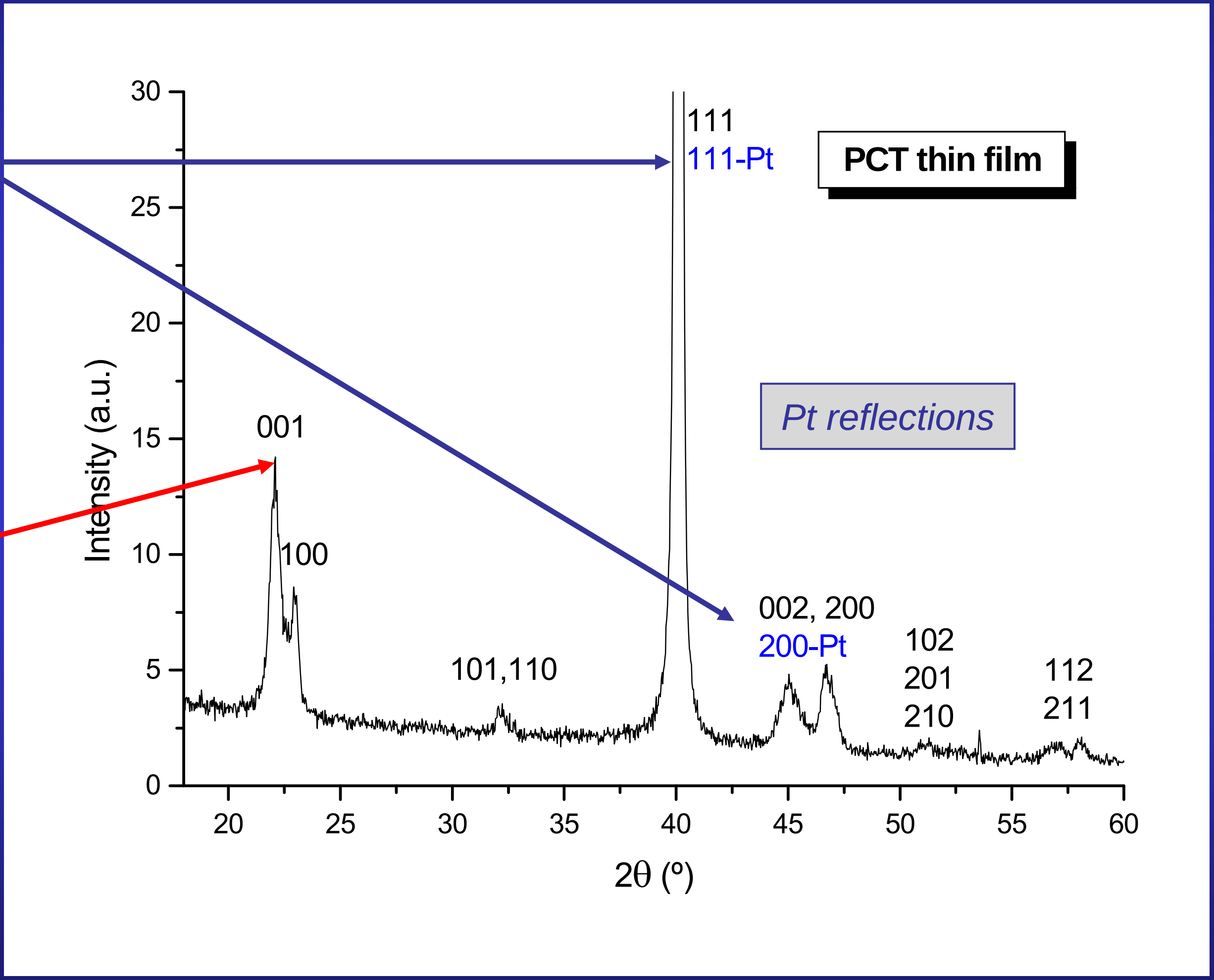

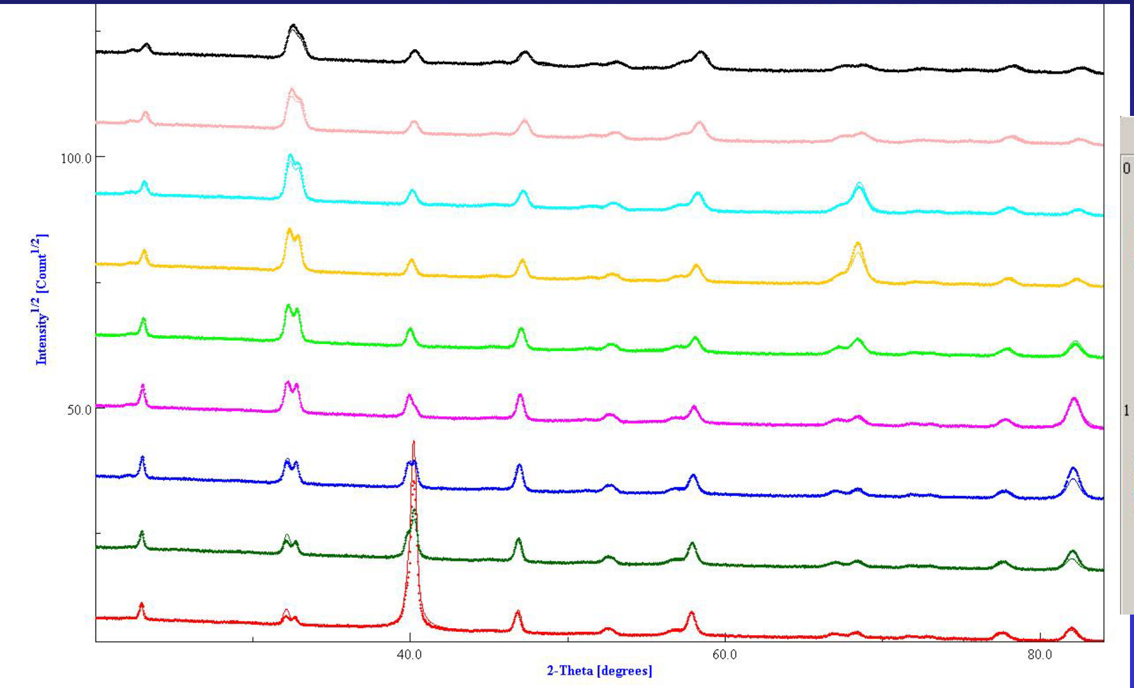

PCT

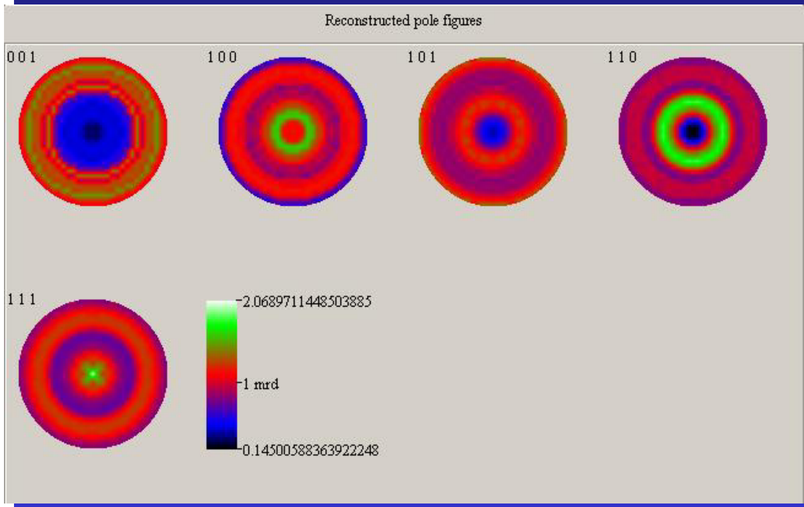

$a = 3.9156(1)$ Å
$c = 4.0497(3)$ Å
$T = 2525(13)$ Å
$t_{iso} = 390(7)$ Å
$\varepsilon = 0.0067(1)$ rms

Pt

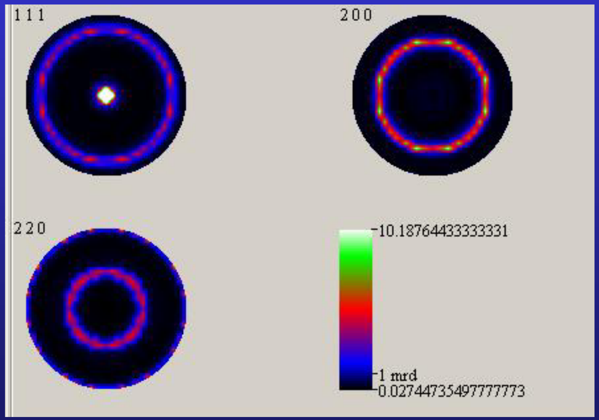

$a = 3.9108(1)$ Å
$T = 457(3)$ Å
$t_{iso} = 458(3)$ Å
$\varepsilon' = 0.0032(1)$ rms

$R_W = 13\%$; $R_B = 12\%$; $R_{exp} = 22\%$.(Rietveld)
$R_W = 5\%$; $R_B = 6\%$ (E-WIMV)

Atom	Occupancy	x	y	z
Pb	0.76	0.0	0.0	0.0
Ca	0.24	0.0	0.0	0.0
Ti	1.0	0.5	0.5	0.477(2)
O1	1.0	0.5	0.5	0.060(2)
O2	1.0	0.0	0.5	0.631(1)

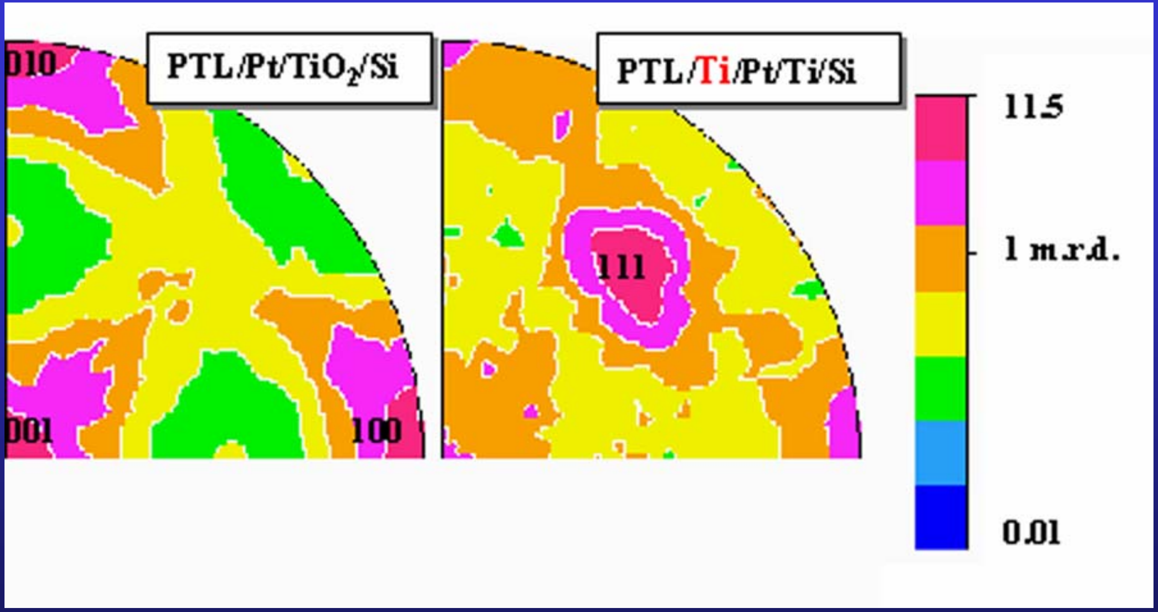

Structural parameters

Pt layer

	a (Å)	thickness (nm)	R factors (%)
non-treated substrate			
Pt	3.9108(1)	45.7(3)	R_W=13, R_B=12, R_{exp}=22
annealed substrate			
Pt	3.9100(4)	46.4(3)	R_W=8, R_B=14, R_{exp}=21
Pt (Recryst. 1h)	3.9114(2)	47.8(3)	R_W=9, R_B=20, R_{exp}=21
Pt (Recryst. 2h)	3.9068(1)	46.9(3)	R_W=9, R_B=14, R_{exp}=22
Pt (Recryst. 3h)	3.9141(4)	47.5(9)	R_W=27, R_B=12, R_{exp}=21

Annealing of the substrate does not introduce significant variations on the structure of the Pt layer

PTC film

	a (Å)	c (Å)	thickness (nm)
on non-treated substrate			
PCT	3.9156(1)	4.0497(6)	272.5(13)
on annealed substrate			
PCT	3.8920(6)	4.0187(8)	279.0(9)
PCT (Recryst. 1h)	3.8929(2)	4.0230(4)	266.1(11)
PCT (Recryst. 2h)	3.8982(2)	4.0227(4)	258.4(9)
PCT (Recryst. 3h)	3.9001(4)	4.0228(11)	253.6(29)

Recrystallisation reduces the stress on the film, and, increases the lattice parameters

Structural, microstructural and texture quantitative characterisation of ferroelectric thin films by the combined method

Analysis of the X-ray diffraction diagrams of a PCT film on $Pt/TiO_2/Si$

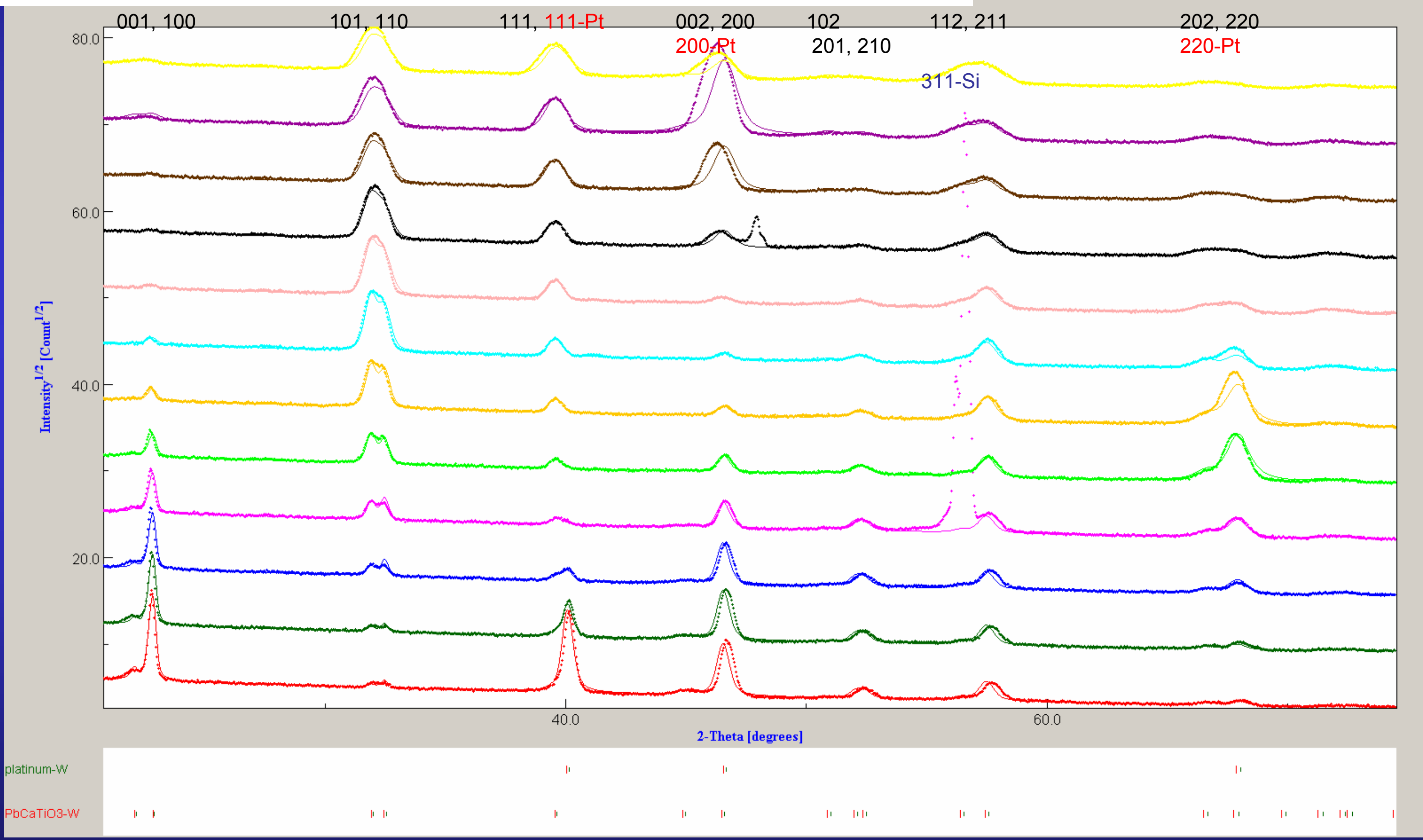

R_W = 13%; R_B = 12%; R_{exp} = 22%.(Rietveld)
R_W = 5%; R_B = 6% (E-WIMV)

Substrate influence on Residual Stress and Texture

Tensile stress

PCT on $Pt/TiO_2/(100)Si$

PCT on $Pt/(100)MgO$

PCT on $Pt/(100)SrTiO_3$

Compressive stress

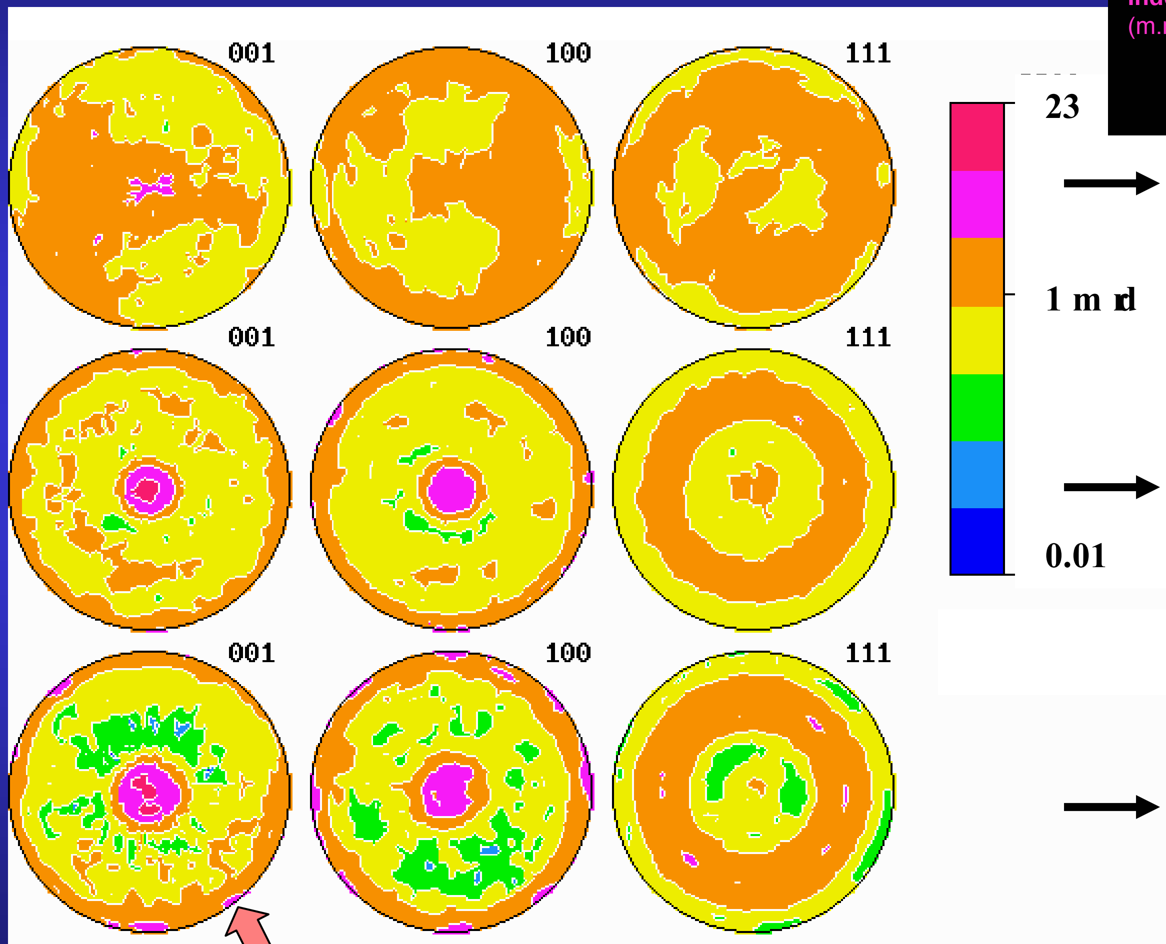

Texture Index (m.r.d.^{2})	Pyroelectric Coefficient (10^{-8}C cm^{-2} K^{-1})
2.1	0.3
5.1	1.5
7.9	1.1

Enhancement of <001> texture

Compliance coefficients [10^{-3} GPa^{-1}]	$PbTiO_3$ single crystal (data set A)	Film random orientation	PCT-Si <001> contrib≈17%	PLT <001> contrib.≈49%	PCT-Mg <001> contrib.≈68%
s_{11}	6.5	10.1	10.5	10.0	9.7
s_{22}	6.5	10.0	10.5	10.0	9.7
s_{33}	33.3	9.8	9.0	10.3	11.3
s_{44}	14.5	13.2	12.8	12.9	13.1
s_{55}	14.5	13.2	12.8	13.0	13.1
s_{66}	9.6	13.4	14.0	13.5	12.7
s_{12}	-0.35	-3.3	-3.5	-3.2	-3.0
s_{21}	-0.35	-3.3	-3.5	-3.2	-3.0
s_{13}	-7.1	-3.2	-3.1	-3.4	-3.6
s_{31}	-7.1	-3.2	-3.1	-3.4	-3.6
s_{23}	-7.1	-3.2	-3.1	-3.4	-3.6
s_{32}	-7.1	-3.2	-3.1	-3.4	-3.6
s_{33}/s_{11}	5.1	0.97	0.86	1.03	1.16
s_{13}/s_{12}	20.3	0.97	0.89	1.06	1.20

Geometric mean average + biaxial stress state

Ferroelectric PMN-PT films

J. Ricote, DMF-Madrid

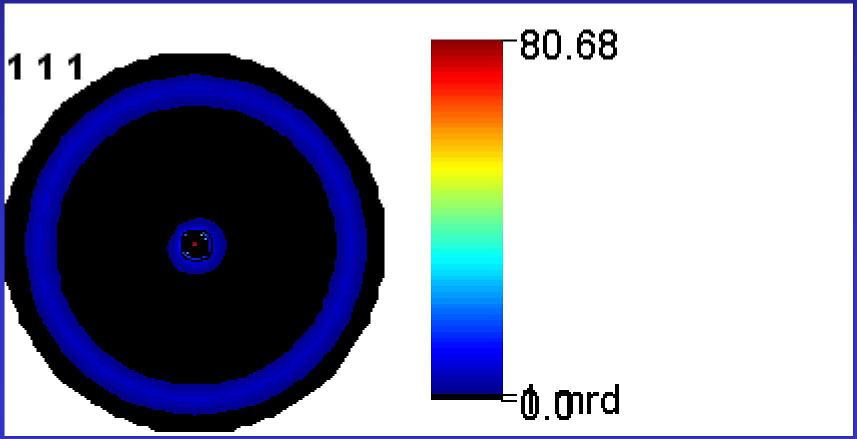

<u>Pt</u>

a = 3.91172(1) Å
T = 583(5) Å
t_{iso} = 960(1) Å
ε = 0.0032(1) rms
σ_{11}= 0.639(1) GPa
σ_{22}= 0.651(1) GPa
σ_{12}= -0.009(1) GPa

$Pb_{0.7}(Mg_{1/3}Nb_{2/3})O_3$-$Pb_{0.3}TiO_3$ /$Ti0_2$/Pt/Si-(100)

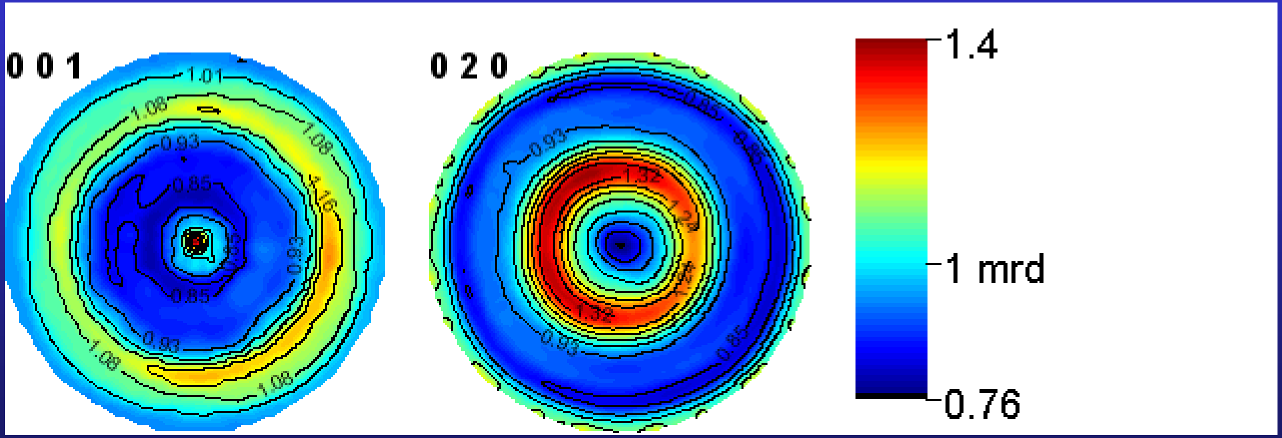

a = 5.67858(9) Å
b = 5.69038(9) Å
c = 3.99558(4) Å
β = 90.392(1) Å
T = 1322(9) Å
t_{iso} = 1338(2) Å
ε = 0.0067(1) rms

$AlN/Pt/TiO_x/Al_2O_3/Ni\text{-}Co\text{-}Cr\text{-}Al$

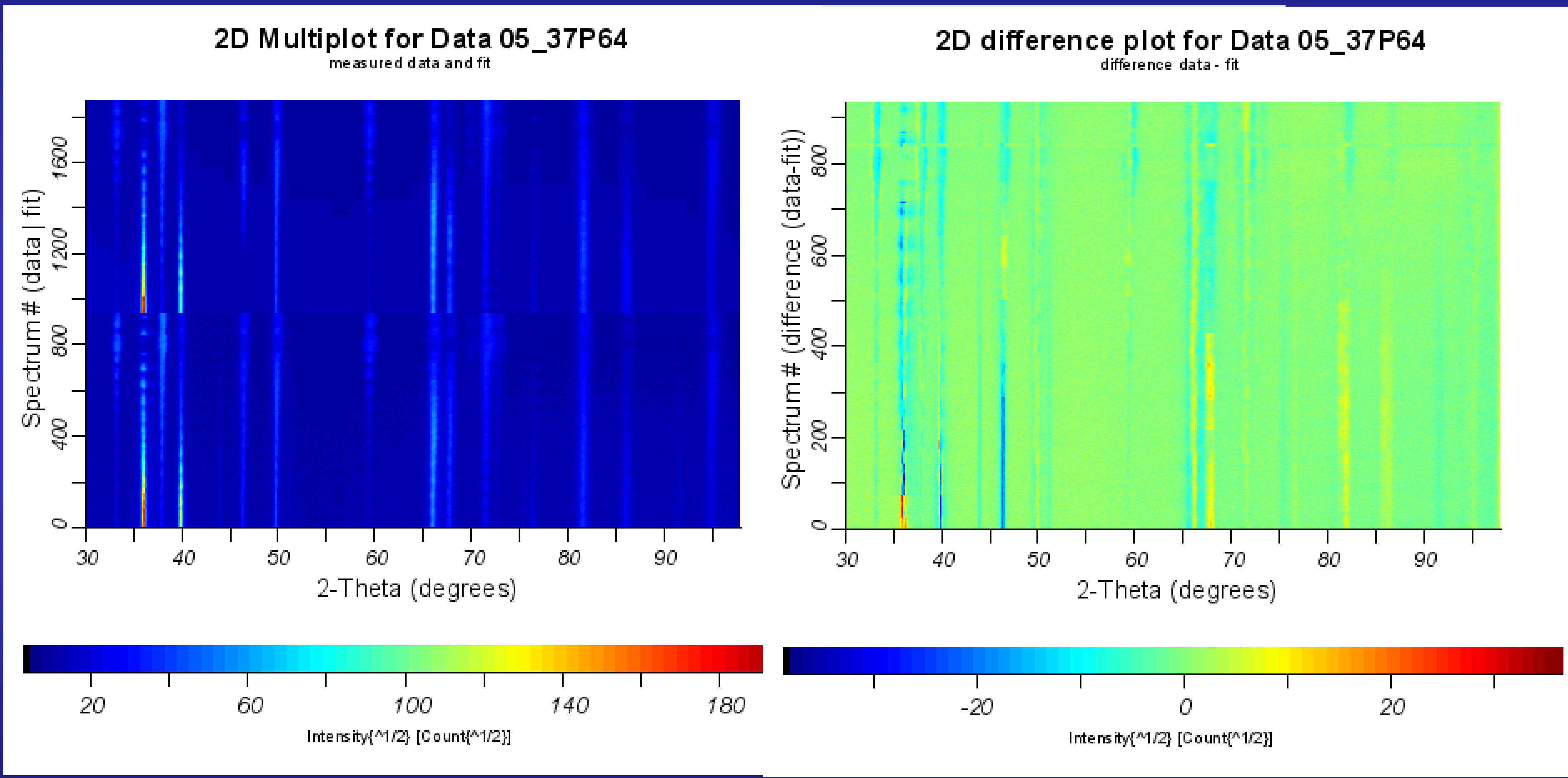

Rw (%) = 24.120445
Rexp (%) = 5.8517213

T(AlN) = 14270(3) nm
T(Pt) = 430(3) nm

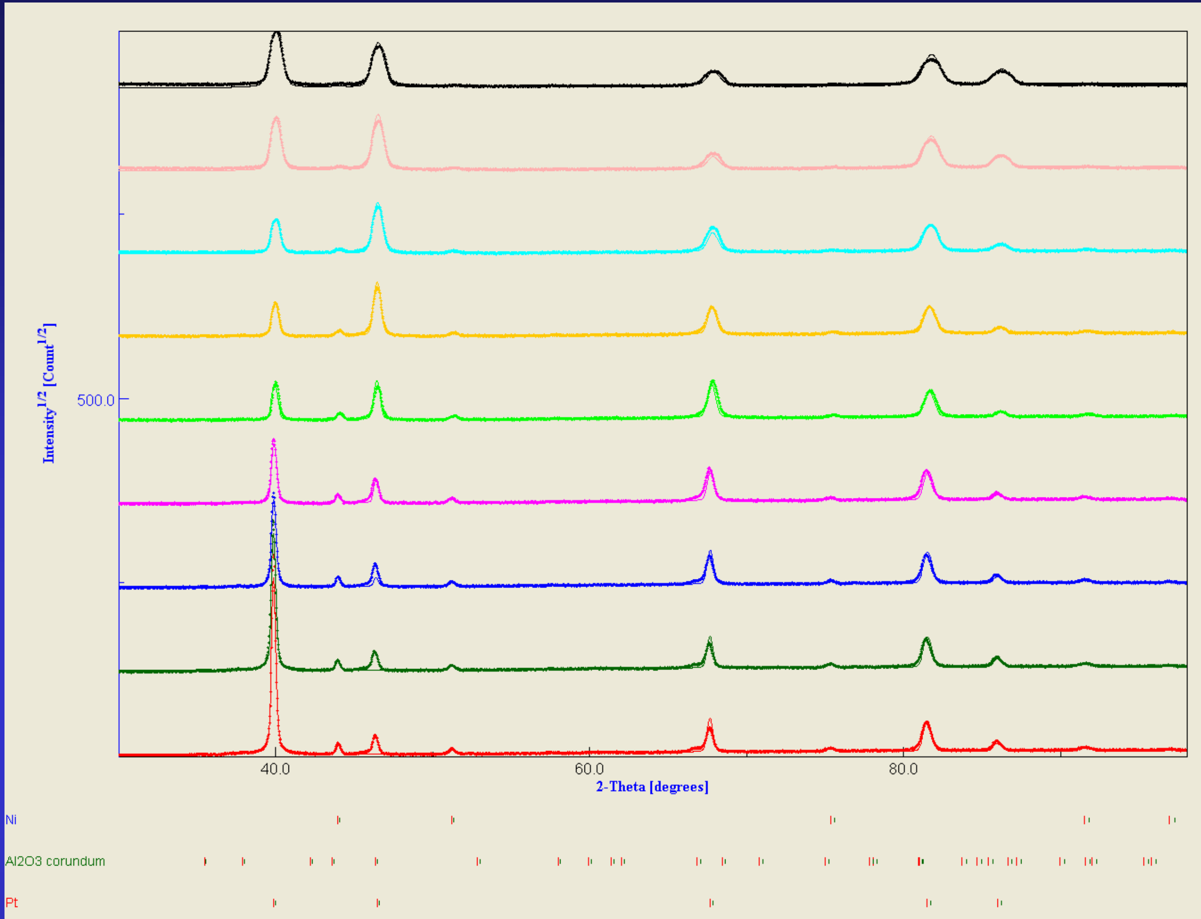

(χ,φ) randomly selected diagrams

Al_2O_3

a = 4.7562(6) Å
c = 12.875(3) Å
T= 7790(31) nm
<t> = 150(2) Å
<ε> = 0.008(3)

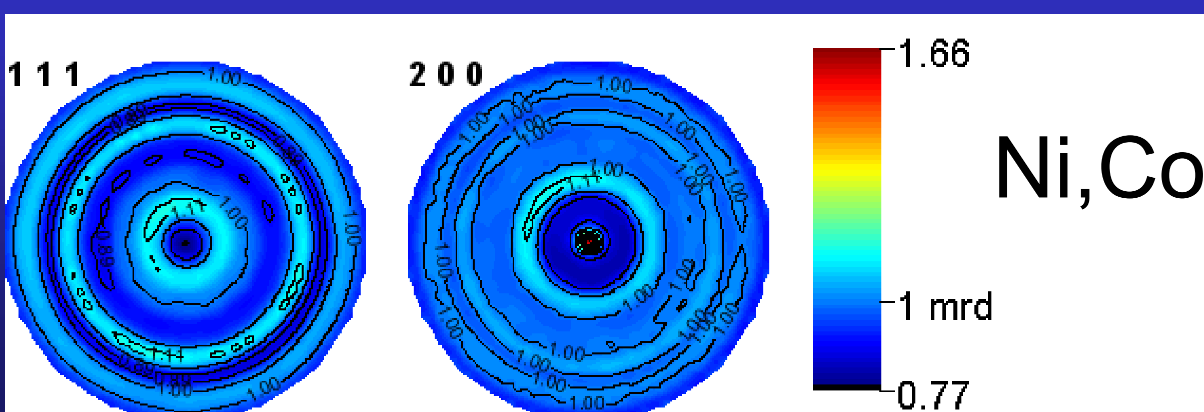

a = 3.569377(5) Å
<t> = 7600(1900) Å
<ε> = 0.00236(3)
σ_{11} = -328(8) MPa
σ_{22} = -411(9) MPa

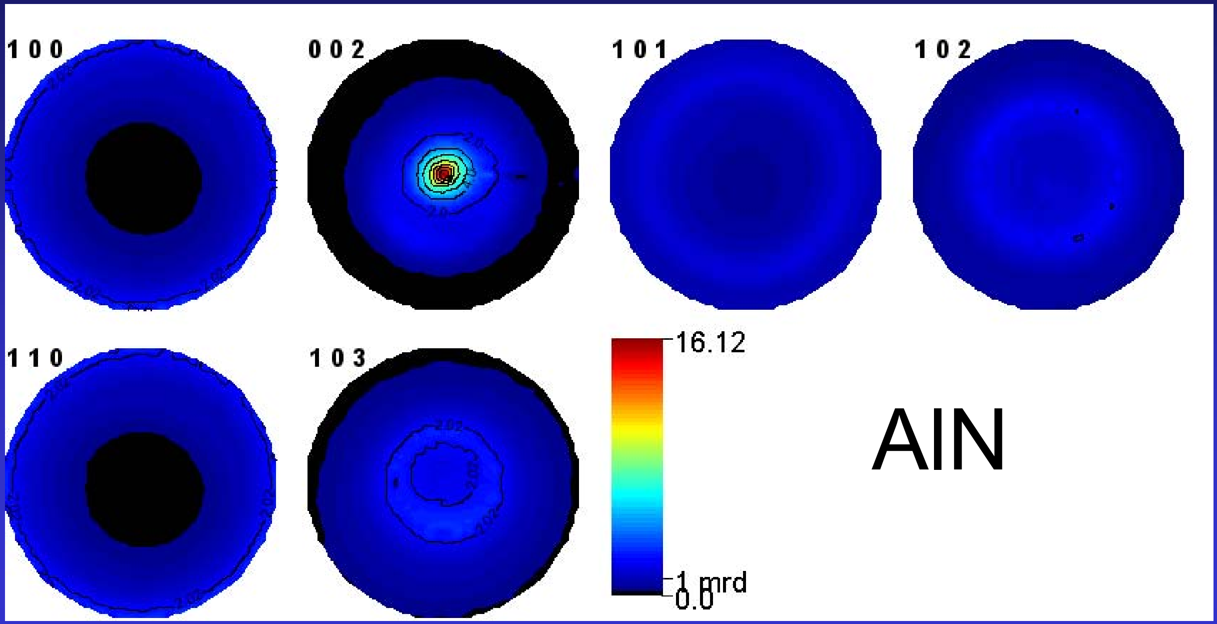

Rw (%) = 4.1

a = 3.11203(1) Å
c = 4.98252(1) Å
T = 14270(3) nm
<t> = 2404(8) Å
<ε> = 0.001853(2)
σ_{11} = -1019(2) MPa
σ_{22} = -845(2) MPa

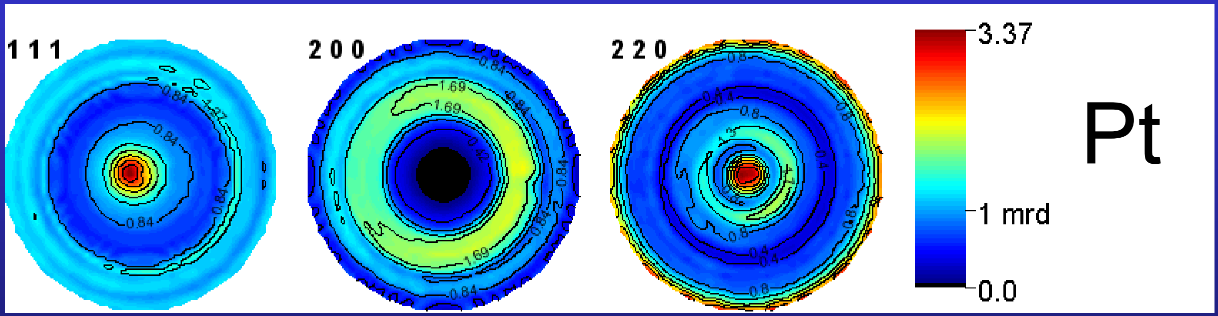

Rw (%) = 33.3

a = 3.91198(1) Å
T = 1204(3) nm
<t> = 2173(10) Å
<ε> = 0.002410(3)
σ_{11} = -196.5(8)
σ_{22} = -99.6(6)

Substrate bias vs stress-texture evolution

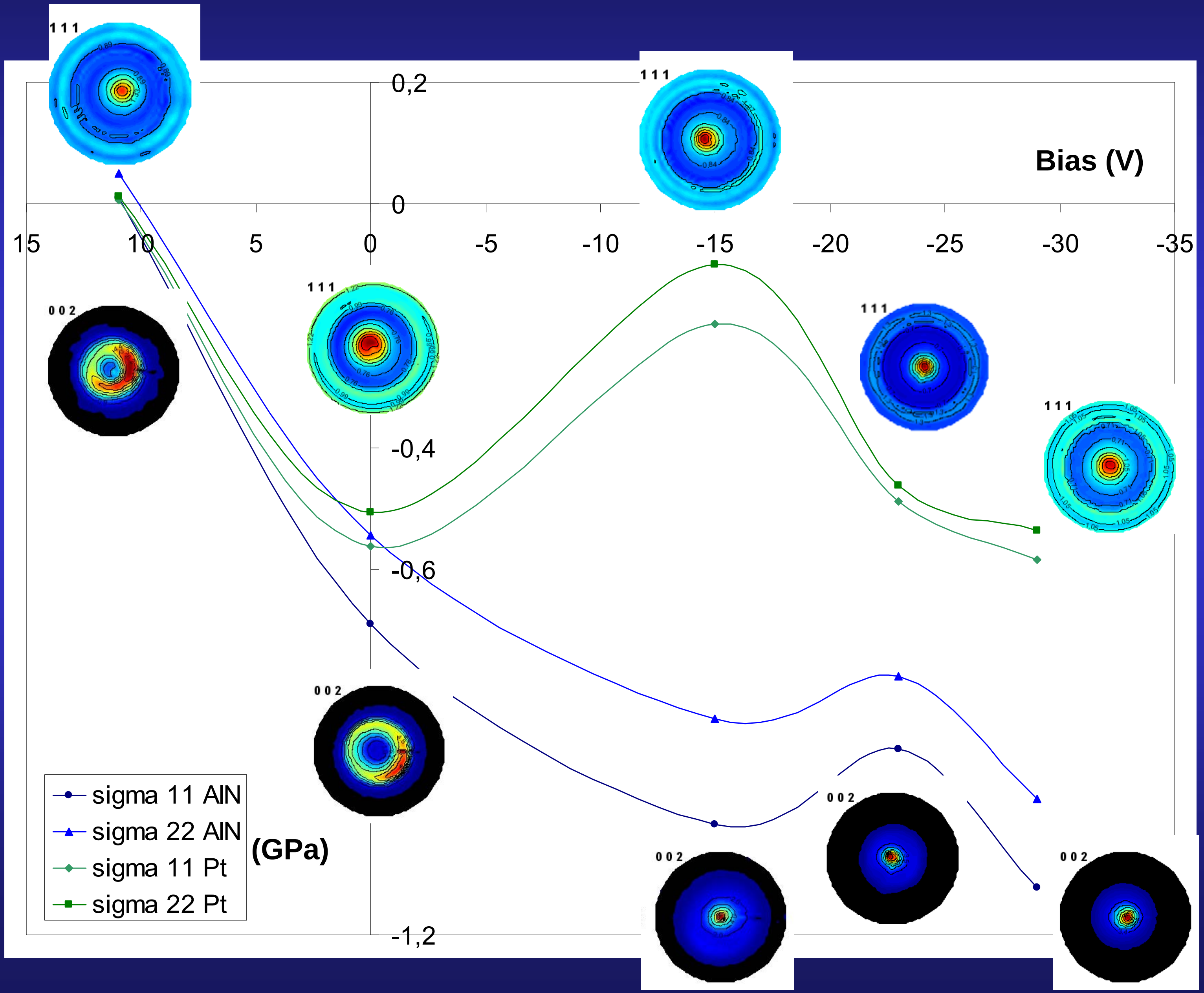

Si nanocrystalline thin films

M. Morales, Caen

Silicon thin films deposition by reactive magnetron sputtering:

- power density 2W/cm^2
- total pressure: $p_{total} = 10^{-1}$ Torr
- plasma mixture: H_2 / Ar, pH_2 / p_{total} = 80 %
- temperature: 200°C
- substrates: amorphous SiO_2 (a-SiO_2)
  (100)-Si single-crystals
- target-substrate distance (d)
  - a-SiO_2 substrates: d = 4, 6, 7, 8, 10, 12 cm
    films A, B, C, D, E, F
  - (100)-Si: d = 6, 12 cm
    films G, H

Aim: quantum confinement, photoluminescence properties

Typical refinement

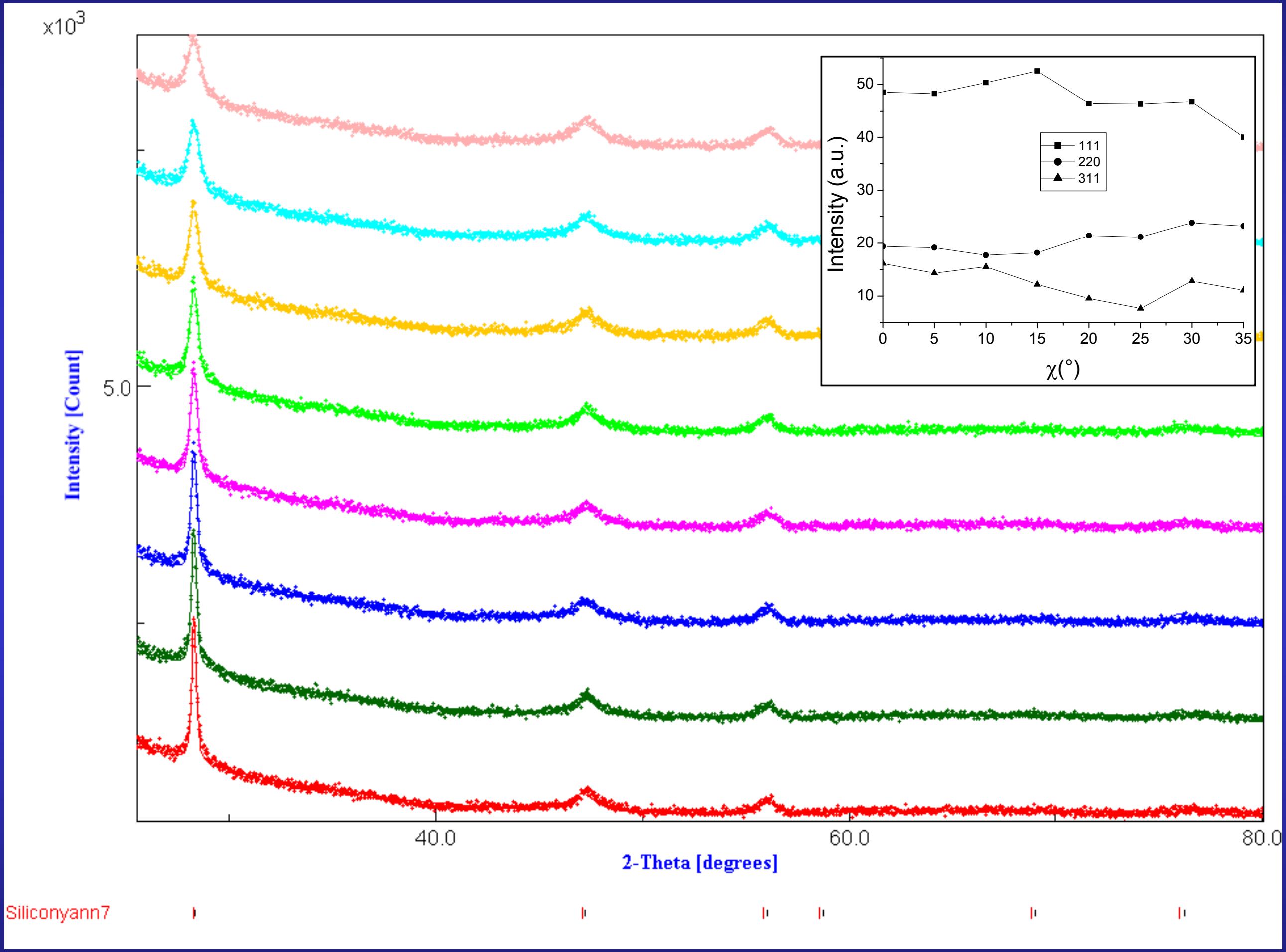

χ = 35°

χ = 0°

broad, anisotropic diffracted lines, textured samples

Refinement Results

Sample	d (cm)	a (Å)	RX thickness (nm)	Anisotropic sizes (Å)			Texture parameters			Reliability factors (%)			
				<111>	<220>	<311>	Maximum (m.r.d.)	minimum (m.r.d.)	Texture index F^2 (m.r.d^2)	RP_0	R_w	R_B	R_{exp}
A	4	5.4466 (3)	---	94	20	27	1.95	0.4	1.12	1.72	4.0	3.7	3.5
B	6	5.4439 (2)	711 (50)	101	20	22	1.39	0.79	1.01	0.71	4.9	4.3	4.2
C	7	5.4346 (4)	519 (60)	99	40	52	1.72	0.66	1.05	0.78	4.3	4.0	3.9
D	8	5.4461 (2)	1447 (66)	100	22	33	1.57	0.63	1.04	0.90	5.5	4.6	4.5
E	10	5.4462 (2)	1360 (80)	98	20	25	1.22	0.82	1.01	0.56	5.0	3.9	4.0
F	12	5.4452 (3)	1110 (57)	85	22	26	1.59	0.45	1.05	1.08	4.2	3.5	3.7
G	6	5.4387 (3)	1307 (50)	89	22	28	1.84	0.71	1.01	1.57	5.2	4.7	4.2
H	12	5.4434 (2)	1214 (18)	88	22	24	2.77	0.50	1.12	2.97	5.0	4.5	4.3

Mean anisotropic shape

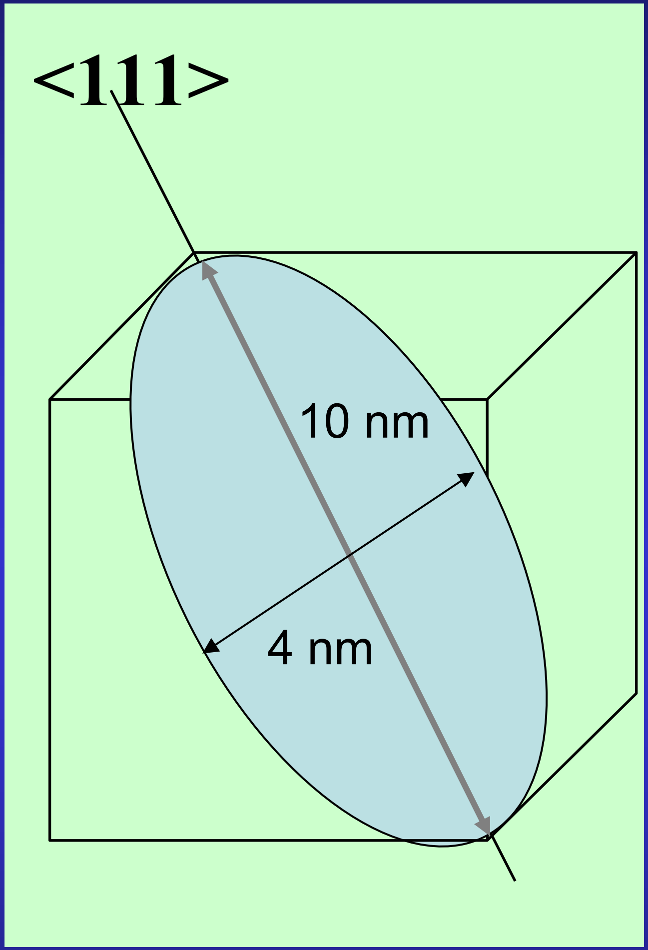

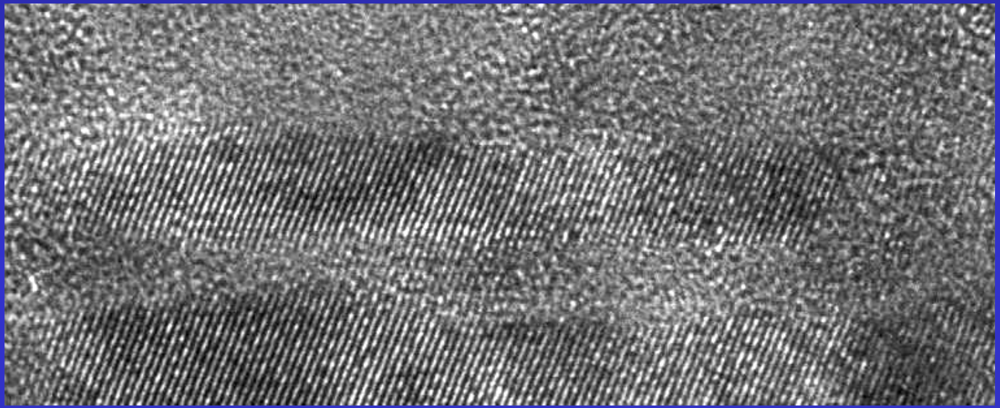

Schematic of the mean crystallite shape for Sample D represented in a cubic cell, as refined using the Popa approach and exhibiting a strong elongation along <111>, and TEM image

001 Inverse Pole Figures

a-SiO_2

(100)-Si

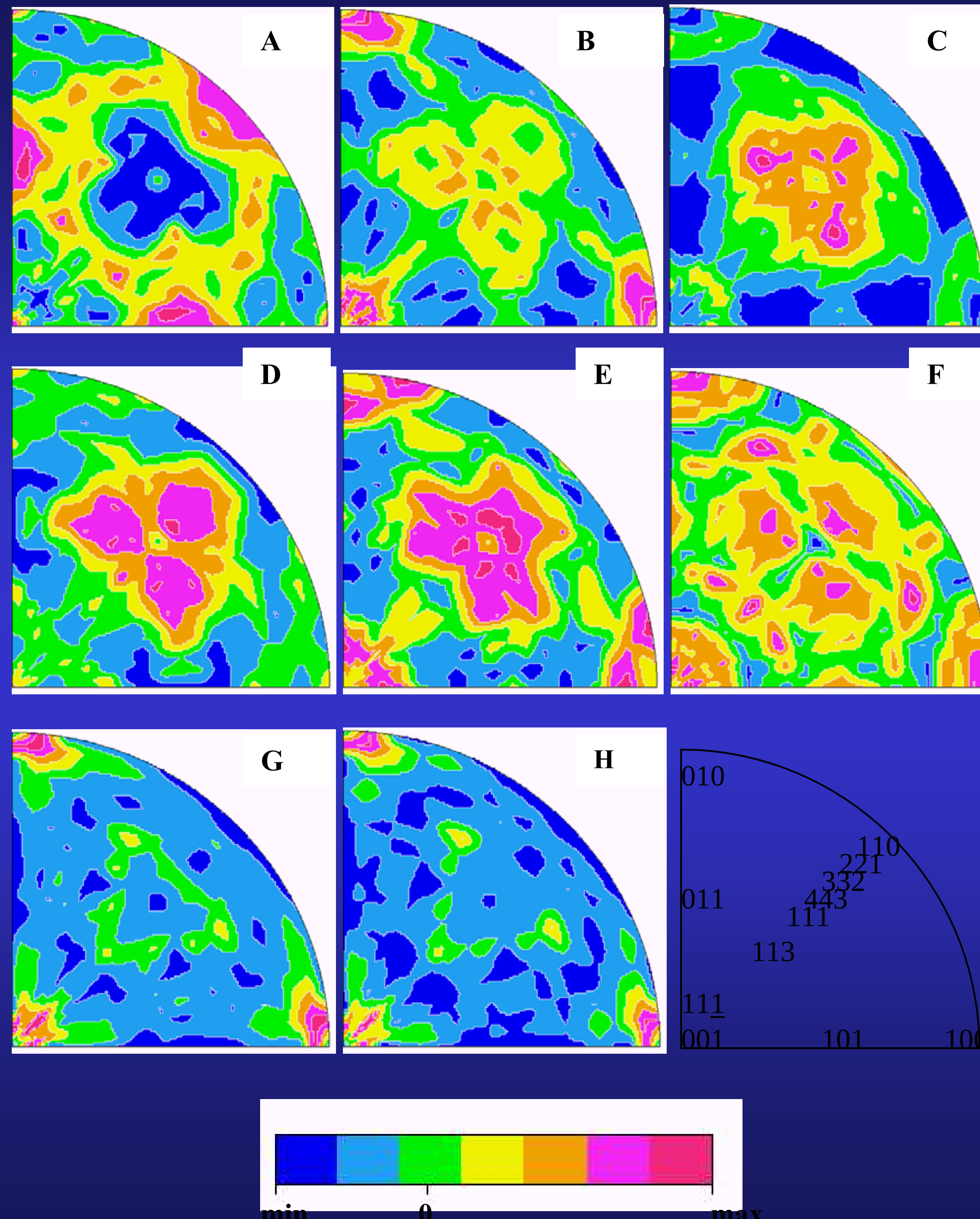

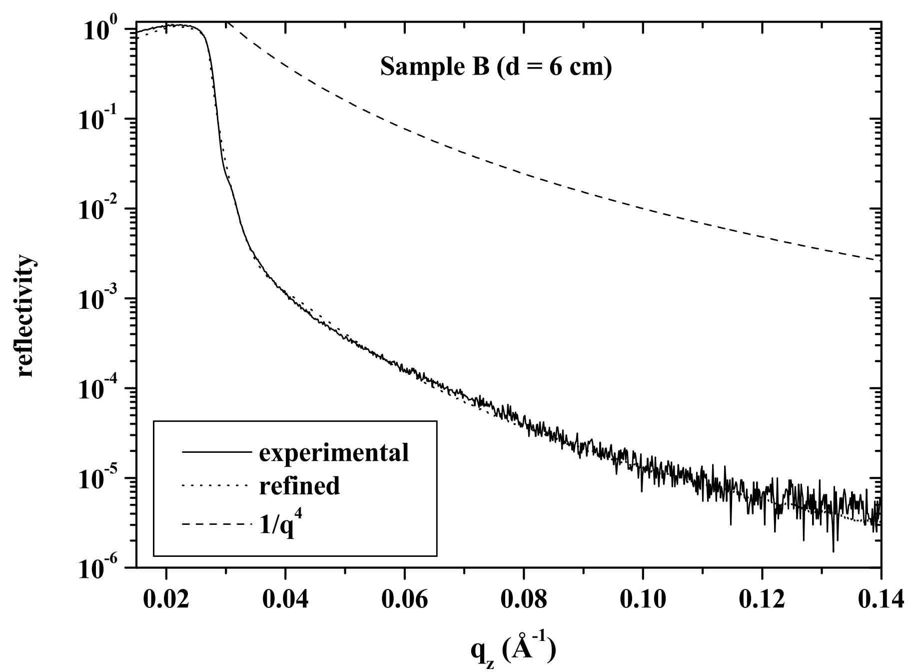

XRR:

Roughness governed

AFM:

homogeneous

roughness

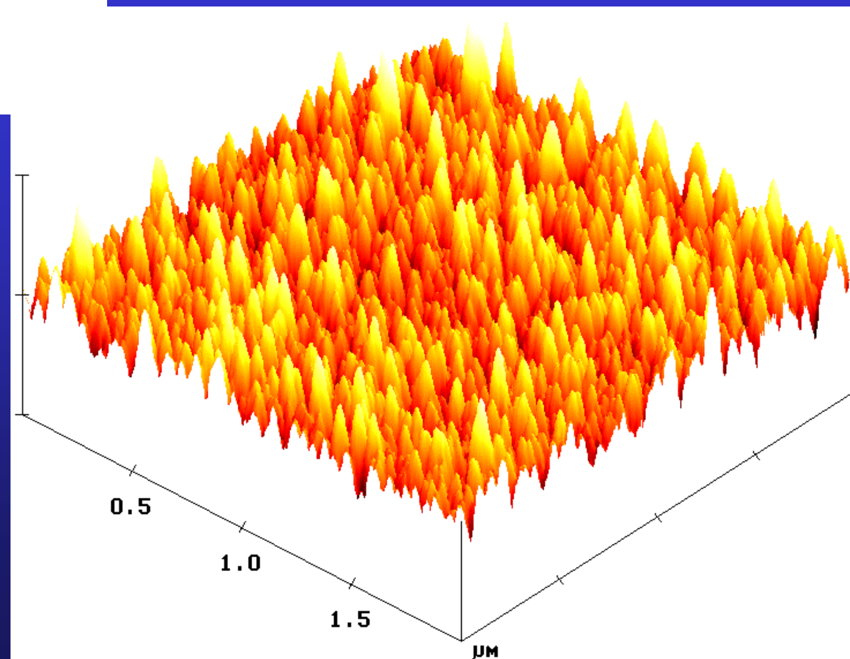

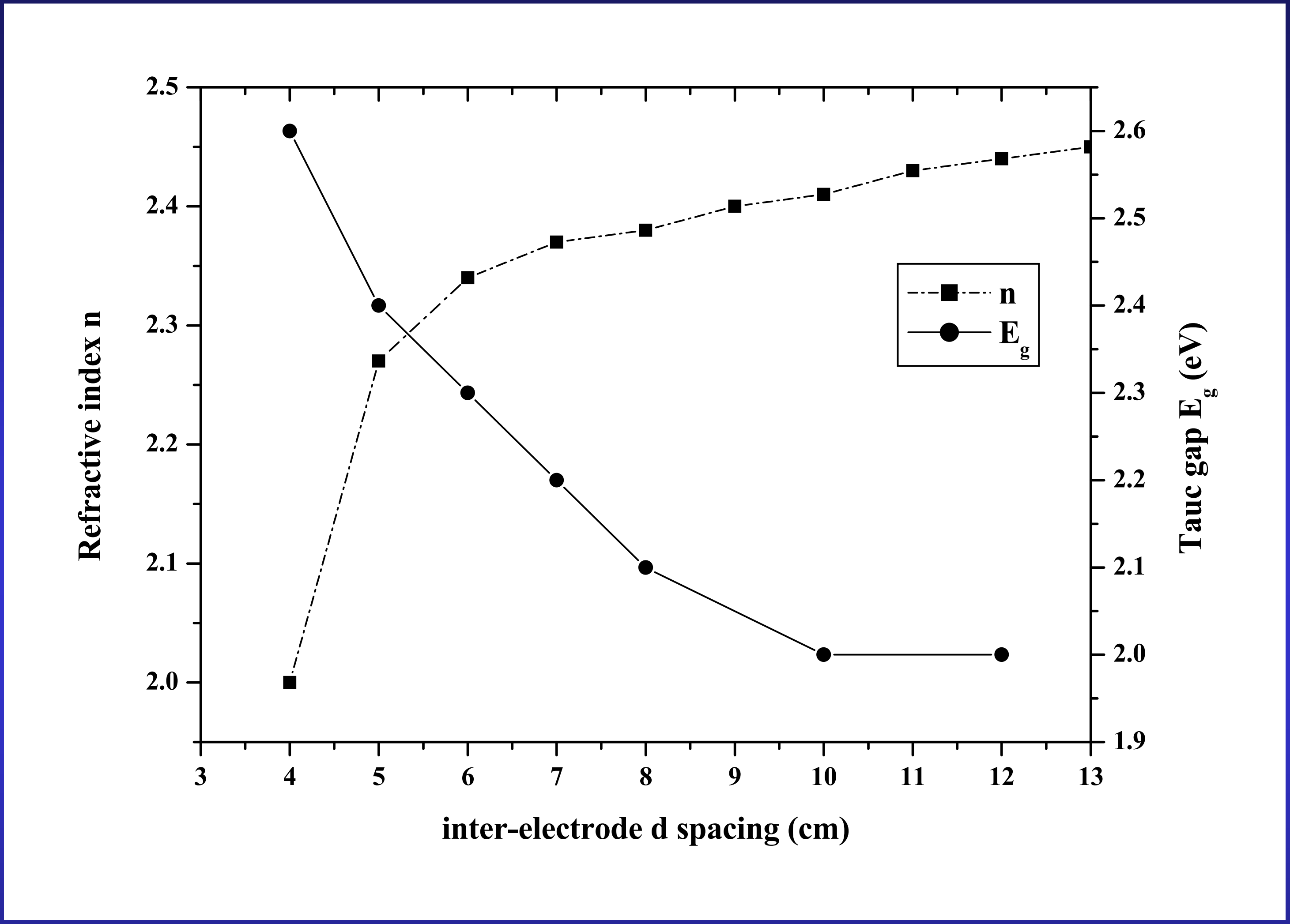

↳ Refractive index linked to film porosities:

Larger target-sample distances: increased compacity due to lower nanopowder filling

Aragonitic layers in mollusc shells

Gastropods

Crossed lamellar layers

Charonia lampas lampas (triton or trumpet cousin)

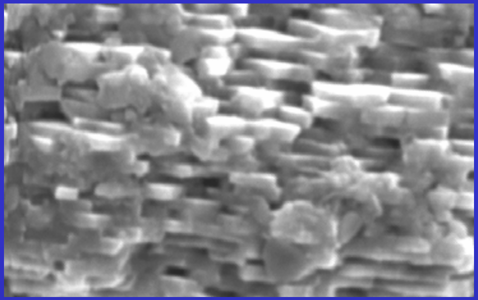

Columnar Nacre

Haliotis tuberculata (common abalone)

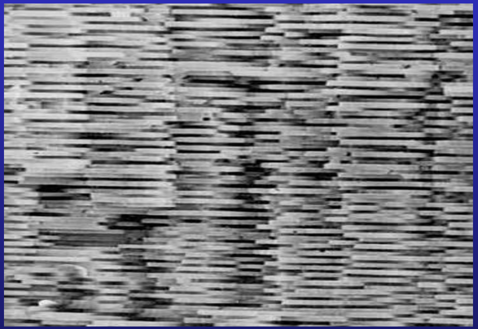

Bivalves

Sheet Nacre

Pinctada maxima (Mother of pearl oyster)

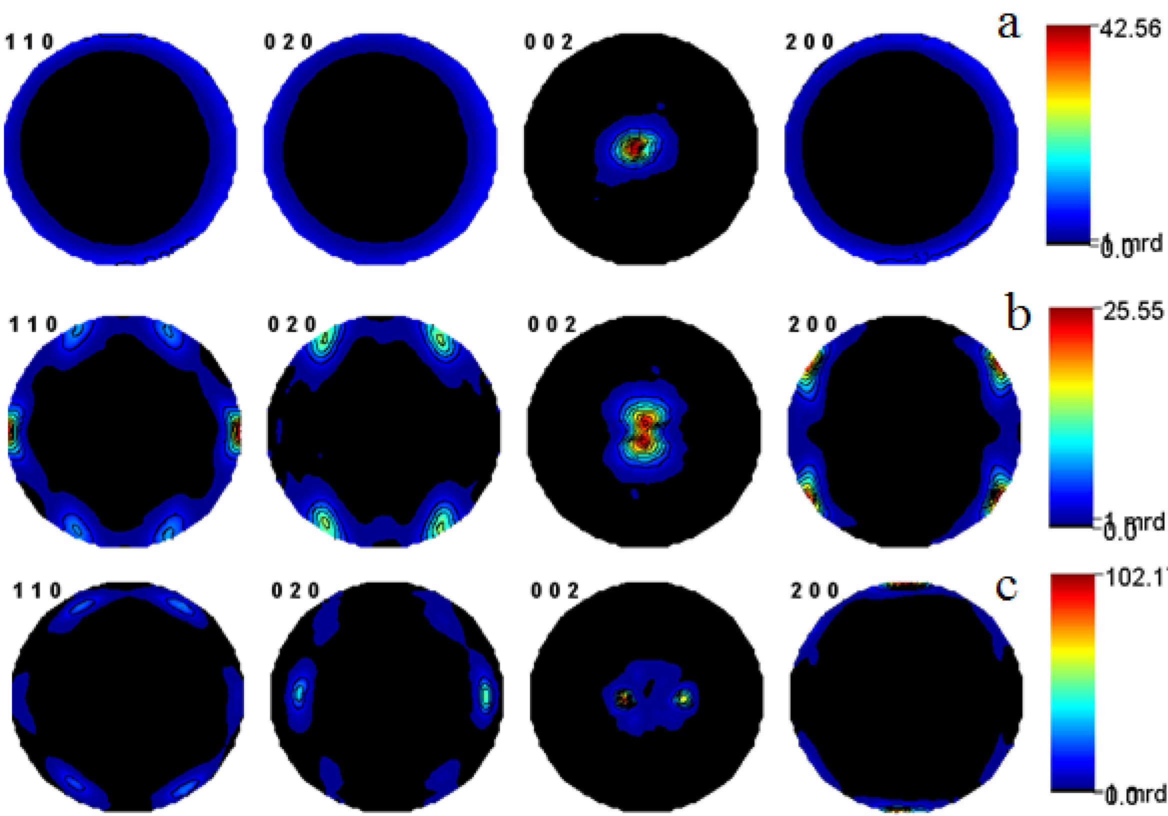

Outer CL
43 mrd^2

Interm Radial CL
47 mrd^2

Inner Com CL
721 mrd^2

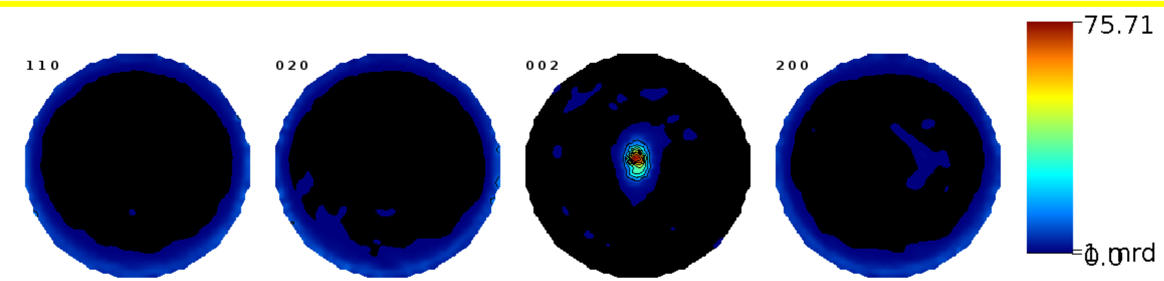

Inner Columnar Nacre
211 mrd^2

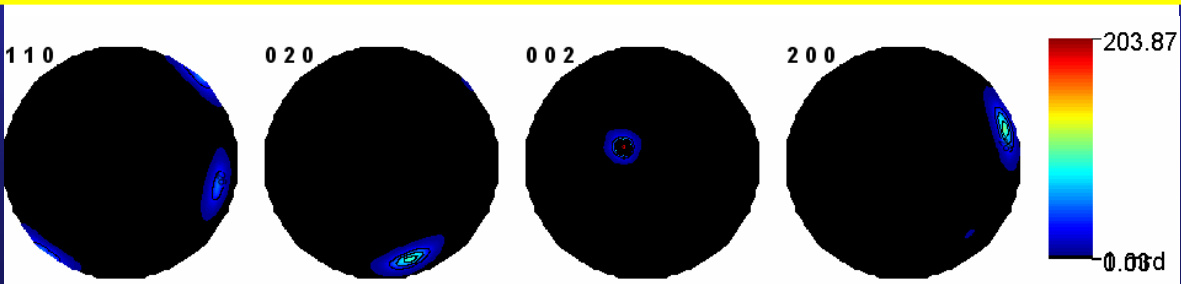

Inner Sheet Nacre
1100 mrd^2

Unit-cell distortions

	OCL	*Charonia* IRCL	ICCL	*Pinctada* ISN	*Haliotis* ICN
a (Å) b (Å) c (Å)	4,98563(7) 8,0103(1) 5,74626(3)	4,97538(4) 7,98848(8) 5,74961(2)	4,9813(1) 7,9679(1) 5,76261(5)	4,97071(4) 7,96629(6) 5,74804(2)	4.9480(2) 7.9427(6) 5.7443(6)
Δa/a Δb/b Δc/c	0,0047 0,0053 0,0004	0,0026 0,0026 0,0010	0,0038 0,0000 0,0033	0.0017 -0.0002 0.0007	-0.0029 -0.0032 0.0007
ΔV/V (%)	1,05	0,62	0,71	0.22	-0.60

Anisotropic cell distortion - depends on the layer

Only nacres exhibit (**a**,**b**) contraction

Due to inter- and intra-crystalline molecules

Distortions and anisotropies larger than pure intra- effect (Pokroy et al. 2007)

Elastic stiffnesses

Single crystal	160	37.3	1.7			
		87.2	15.7			
			84.8			
				41.2		
					25.6	
						42.7
	96.5	31.6	13.7			
		139	9.5			
			87.8			
ICCL				29.8		
					36.6	
						40.2
	130.1	32.6	10.3			
		103.3	14.1			
			84.5			
RCL				36.3		
					31.1	
						40.5
	111.1	32.9	13.2			
		119	11.8			
			84.8			
OCL				32.8		
					34.6	
						40.9

Structural distortions in aragonitic biogenic ceramic composites

Aplanarity of carbonate groups in $CaCO_3$

$$\Delta Z_{C\text{-}O1} = c(z_C - z_{O1})$$

Calcite	Biogenic aragonite	Mineral aragonite
0 Å	*Intermediate ?*	*0.05744 Å*

Atomic Structures

		Geological reference	*Charonia lampas* OCL	*Charonia lampas* IRCL	*Charonia lampas* ICCL	*Strombus decorus* mixture	*Pinctada maxima* ISN
Ca	y z	0.41500 0.75970	0.41418(5) 0.75939(3)	0.414071(4) 0.76057(2)	0.41276(9) 0.75818(8)	0.4135(7) 0.7601(8)	0.41479 (3) 0.75939 (2)
C	y z	0.76220 -0.08620	0.7628(2) -0.0920(1)	0.76341(2) -0.08702(9)	0.7356(4) -0.0833(2)	0.7607(4) -0.0851(7)	0.7676 (1) -0.0831 (1)
O1	y z	0.92250 -0.09620	0.9115(2) -0.09205(8)	0.9238(1) -0.09456(6)	0.8957(3) -0.1018(2)	0.9228(4) -0.0905(9)	0.9134 (1) -0.09255 (7)
O2	x y z	0.47360 0.68100 -0.08620	0.4768(1) 0.6826(1) -0.08368(6)	0.4754(1) 0.68332(9) -0.08473(5)	0.4864(3) 0.6834(2) -0.0926(1)	0.4763(6) 0.6833(3) -0.0863(7)	0.4678 (1) 0.68176 (7) -0.09060 (4)
$\Delta Z_{C\text{-}O1}$ (Å)		**0.05744**	**0.00029**	**0.04335**	**0.1066**	**0.031**	**0,054**

Carbonate group aplanarity specific to a given layer

Aplanarity decreases from inner to outer shell layers (CL layers)

-> up to quite ΔZ=0 outside (nearly the calcite value)

Average aplanarity on the whole shell = geological reference (Strombus)

In Haliotis nacre: large ΔZ=0.08, + strong anisotropy: less stable nacre

Irradiated FluorApatite (FAp) ceramics

Self-recrystallisation under irradiation, depending on SiO_4 / PO_4 ratio (FAp / Nd-Britholite) and on irradiating species

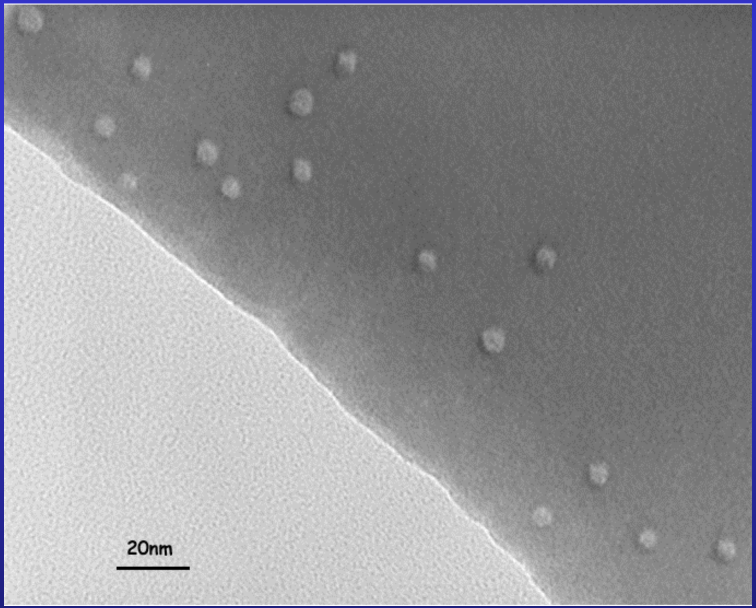

TEM of FAp irradiated with 70 MeV, 10^{12} Kr cm^{-2} ions

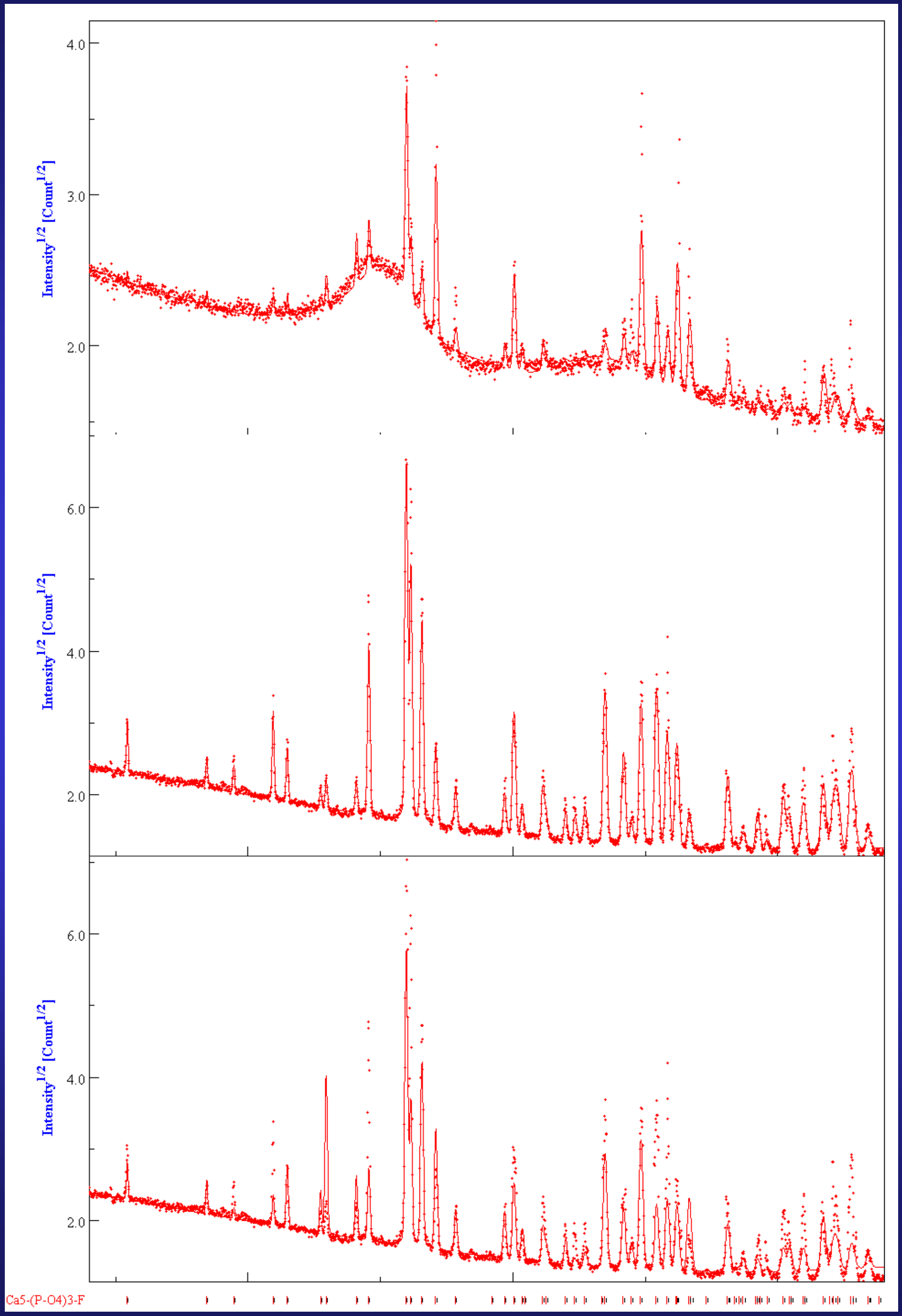

texture corrected,

10^{13} Kr cm^{-2}

Virgin, with texture correction

Virgin, no texture correction

Fluence (ions.cm^{-2})	Vc/V (%)	A (Å)	c (Å)	<t> (nm)	$\Delta a/a_0$ (%)	$\Delta c/c_0$ (%)	R_w (%)	R_B (%)
0	100	9.3365(3)	6,8560(5)	294(22)	-	-	14.6	9.1
Kr								
10^{11}	100	-	-	-	-	-		
10^{12}	100	-	-	-	-	-		
5.10^{12}	49(1)	9.3775(9)	6.8912(8)	294(20)	0.44	0.53	24	15
10^{13}	20(1)	9.4236(5)	6.9105(5)	291(20)	0.94	0.82	9.9	6
5.10^{13}	14(1)	9.3160(4)	6.8402(5)	294(22)	-0.21	-0.22	10.5	5.9
I								
10^{11}	-	-	-	-	-	-		
5.10^{11}	86(2)	9.3603(3)	6.8790(5)	90(10)	0.26	0.35	23.9	15.1
10^{12}	-	-	-	-	-	-		
3.10^{12}	47(2)	9.3645(3)	6.8840(5)	91(6)	0.30	0.42	13.3	9
5.10^{12}	29.2(5)	9.3765(5)	6.8881(6)	77(11)	0.44	0.48	10.4	7.3
10^{13}	13.2(2)	9.3719(4)	6.8857(6)	82(9)	0.38	0.45	6.7	4.9

Single impact model associated to crystal size reduction

Cell parameters and volume increase, then relax

Amorphisation / recrystallisation competition: single or double impact

Amorphous/crystalline volume fraction (damaged fraction Fd = Va / V) as determined by x-ray diffraction

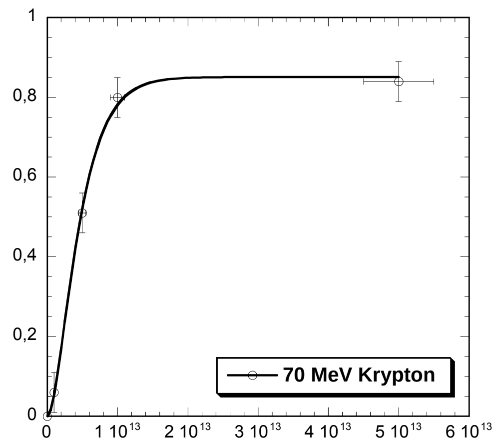

B

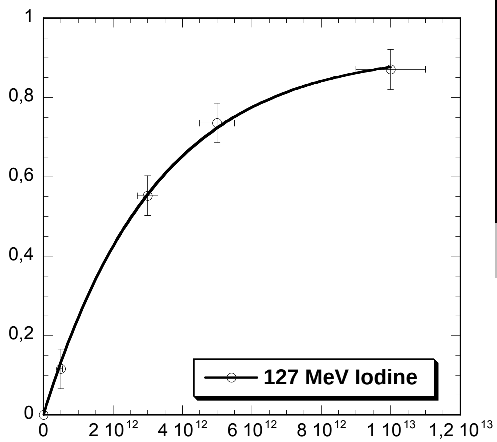

Fitting parameters	Krypton		Iodine
	Single impact	Double impact	Single impact
	Fd = B(1- exp(-Aϕt))	Fd = B(1 – (1+ Aϕt) exp(-Aϕt))	Fd = B(1- exp(-Aϕt))
A = πR^2 (cm^2)	$1.85 \pm 0.15\ 10^{-13}$	$4.1 \pm 0.15\ 10^{-13}$	$3.3 \pm 0.15\ 10^{-13}$
Radius R (nm)	2.4 ± 0.2	3.6	3.2
B (Max.damage rate)	0.87	0.85 ± 0.2	0.92 ± 0.2
$\chi 2$	0.013	0.0006	0.0004

Mullite-silica composites

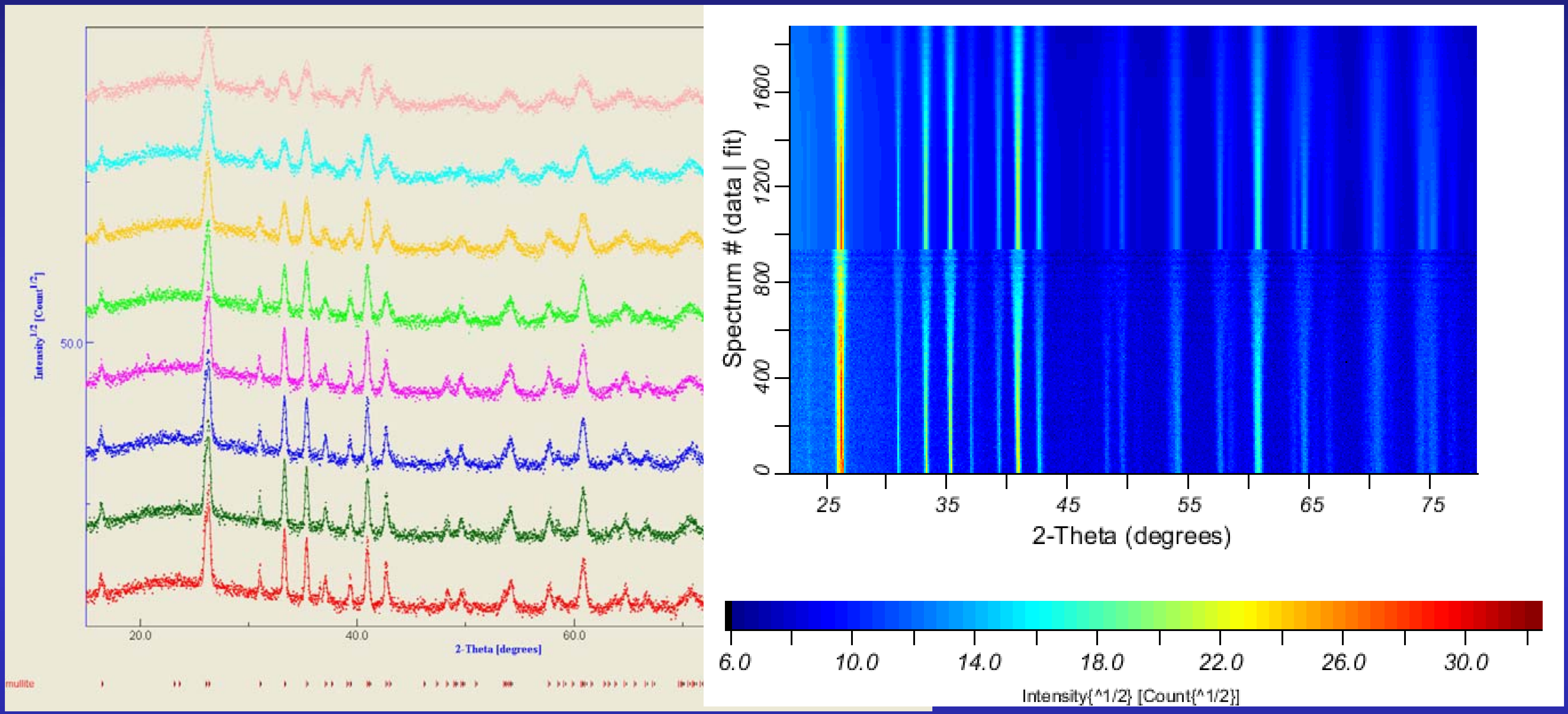

ODF: R_w = 4.87 %, R_B = 4.01 %
Rietveld: R_w = 12.90 %, GoF = 1.77
Mullite: a = 7.56486(5) Å; b = 7.71048(5) Å; c = 2.89059(1)Å

Uniaxially pressed

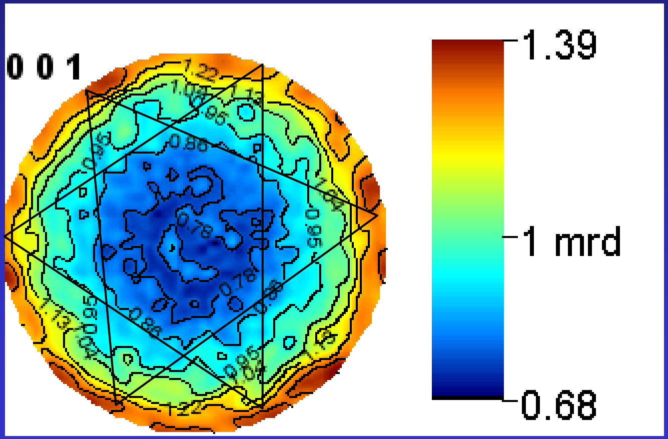

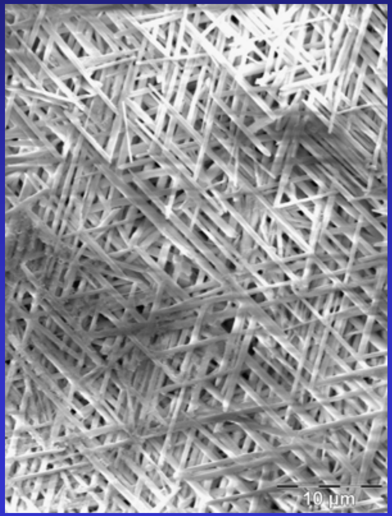

Centrifugated

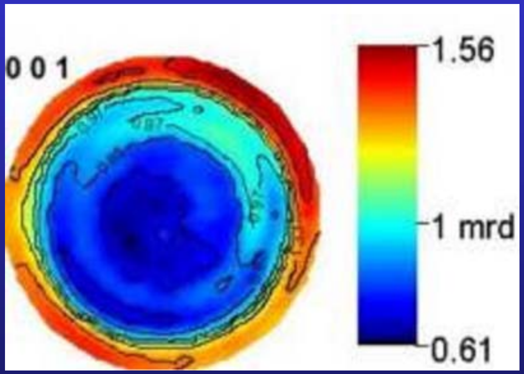

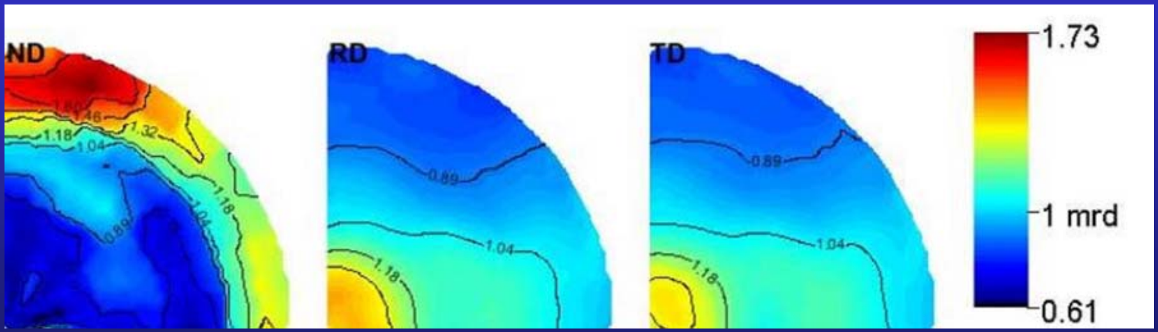

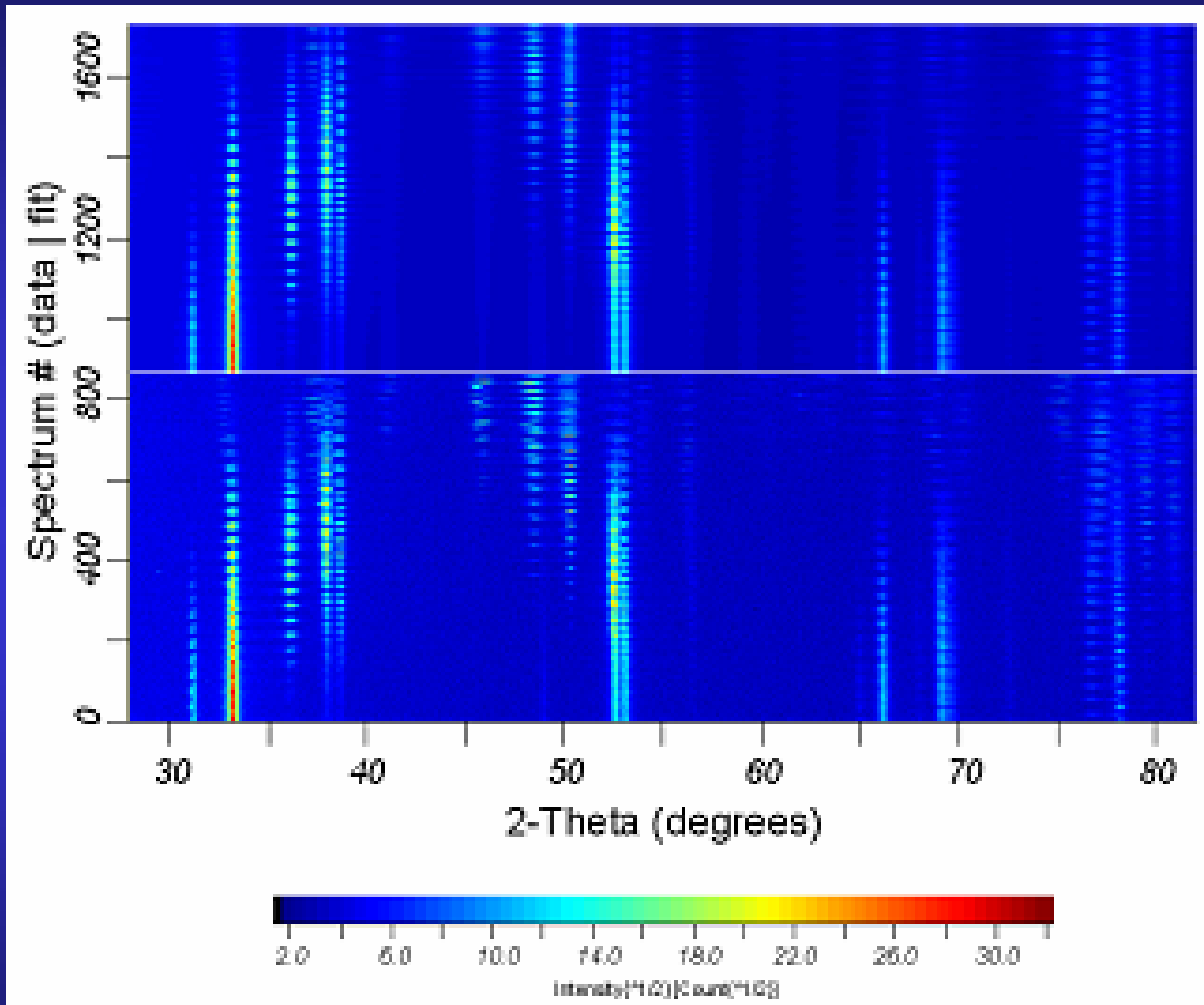

refined

experiments

GoF:1,72
Rw: 28,0%
Rexp:21,3%

for all (χ,φ) sample orientations

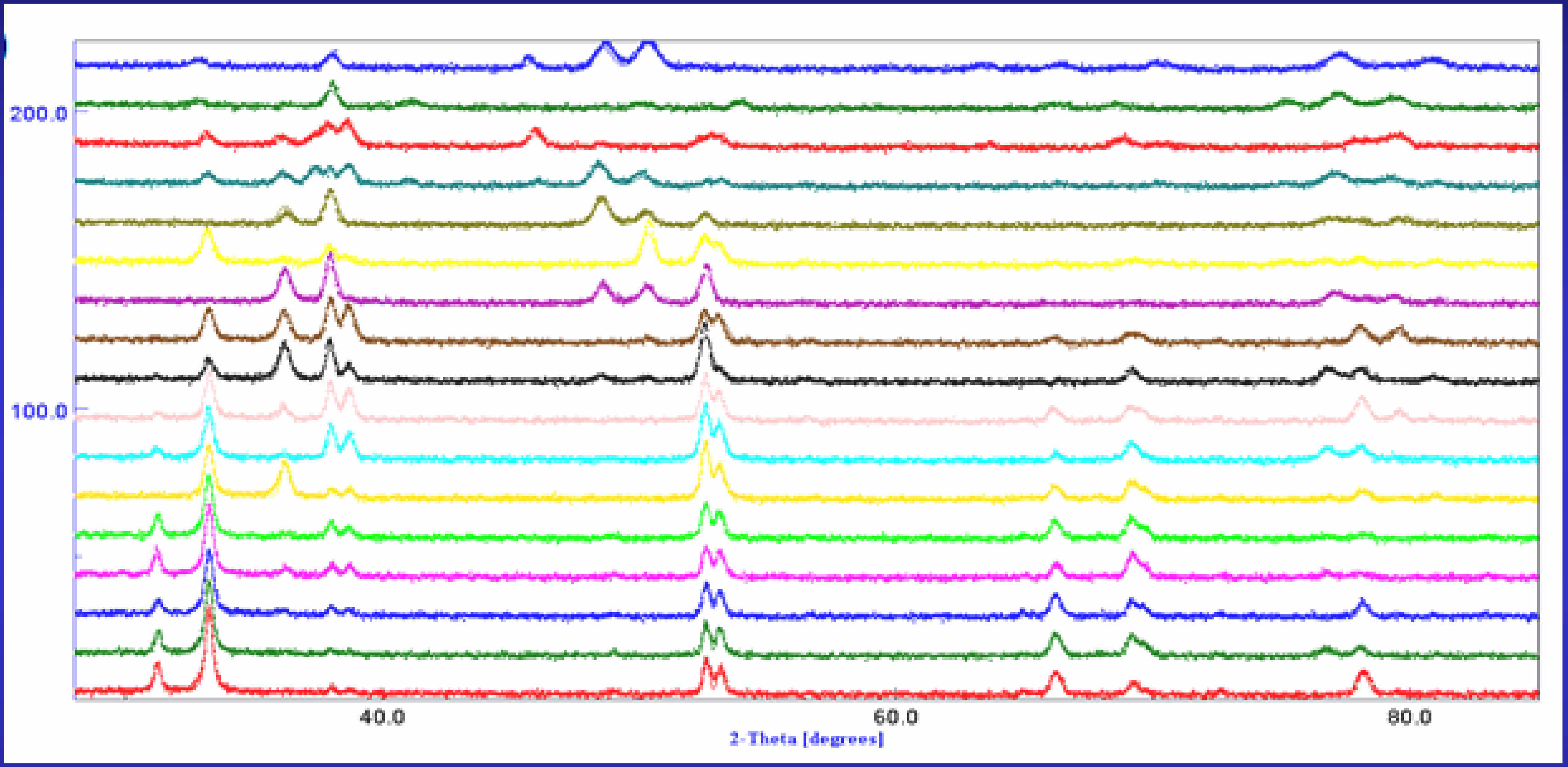

IRC layer of *Charonia lampas lampas* for selected (χ,φ) sample orientations

Turbostratic phyllosilicate aggregates

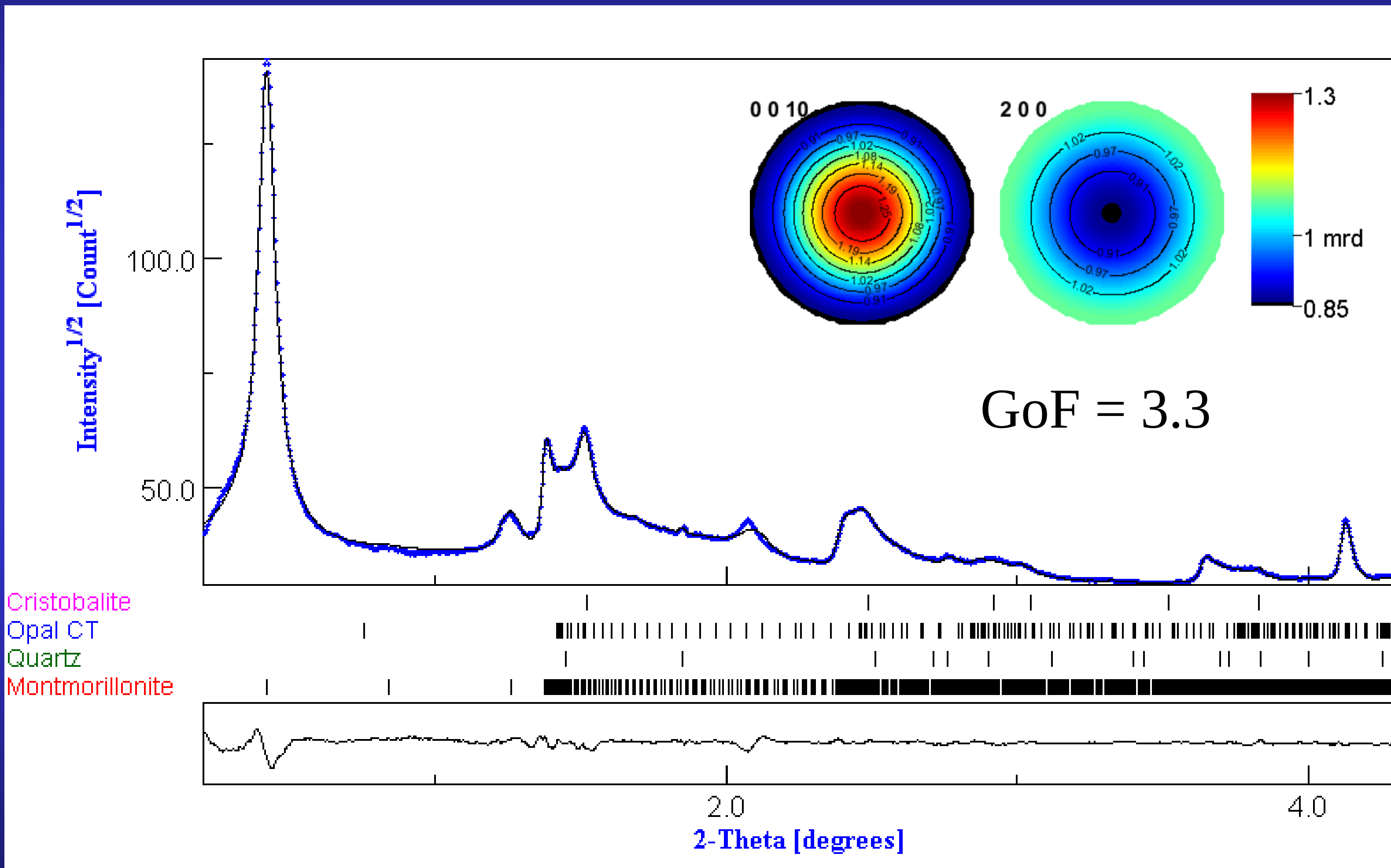

V%
1.45(2)
6.6(1)
0.19(1)
91.8(3)

Al_2O_3 « standard » powder

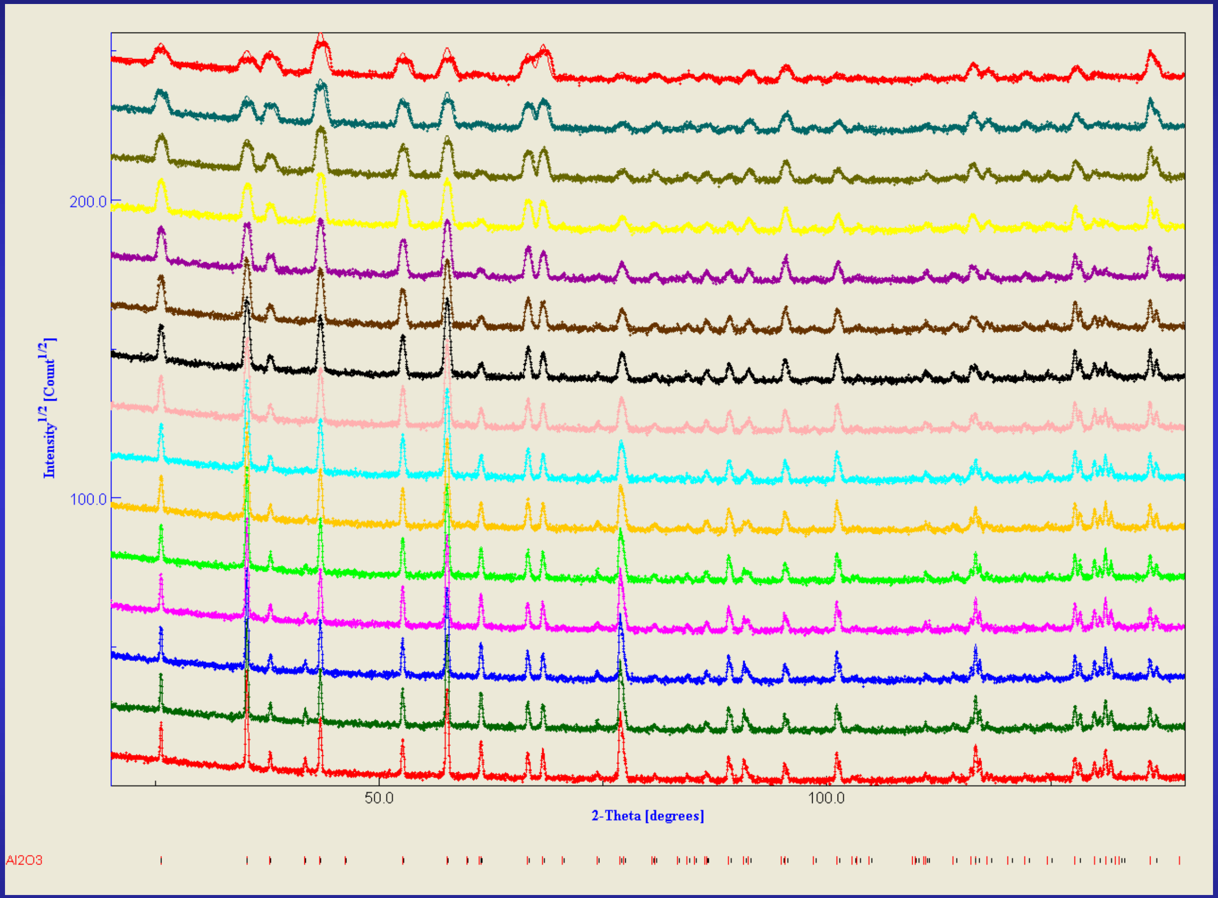

<u>2θ-scans:</u>
GoF = 1.92
R_W = 15.60 %
R_B = 11.94 %

<u>θ–2θ-scans:</u>
GoF = 1.86
R_W = 16.11 %
R_B = 12.40 %

15 diagrams x 5 mn (fibre texture): 1.25 h
936 diagrams x 5 mn (non symmetric texture): 3.25 days

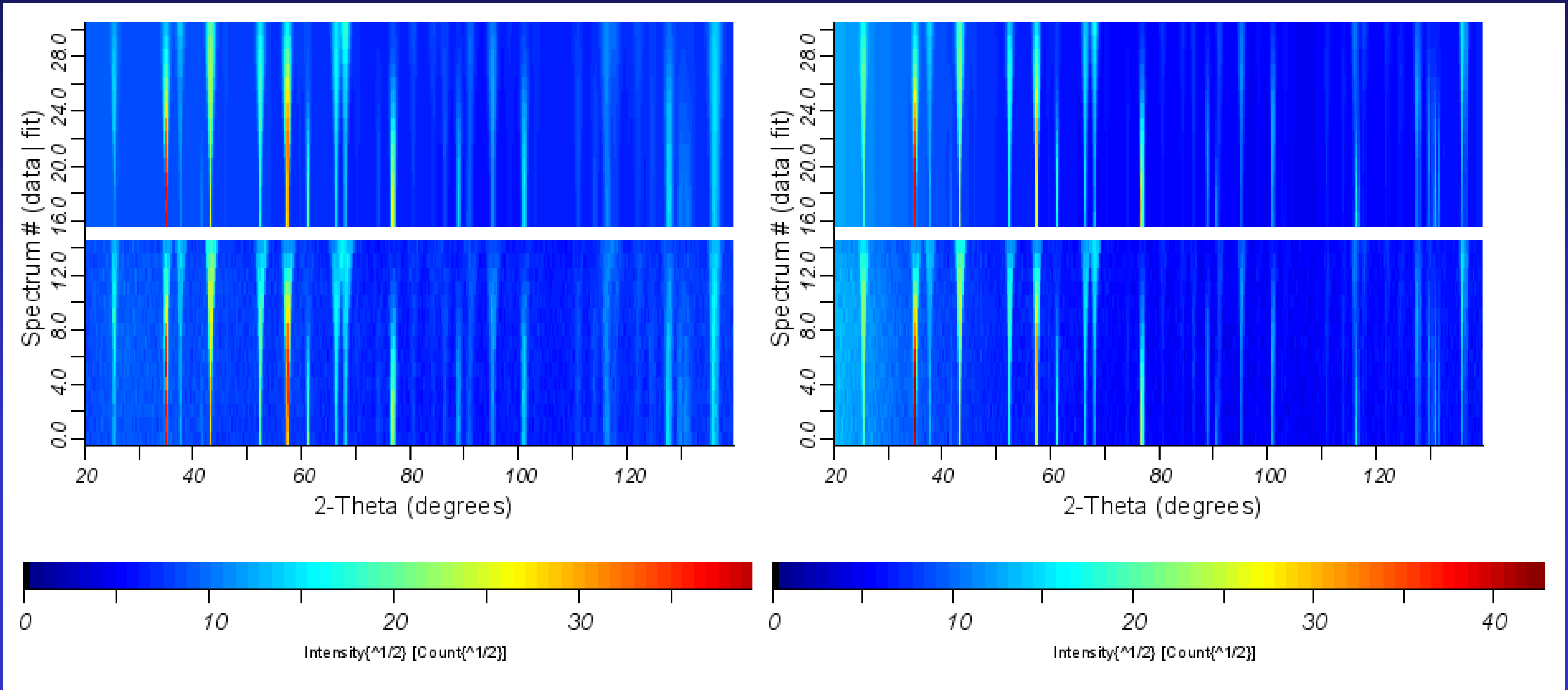

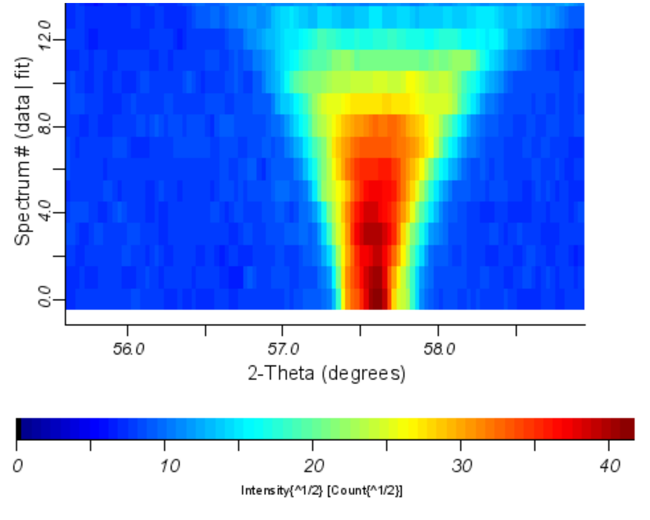

-70 microns x shift in χ
And texture !!

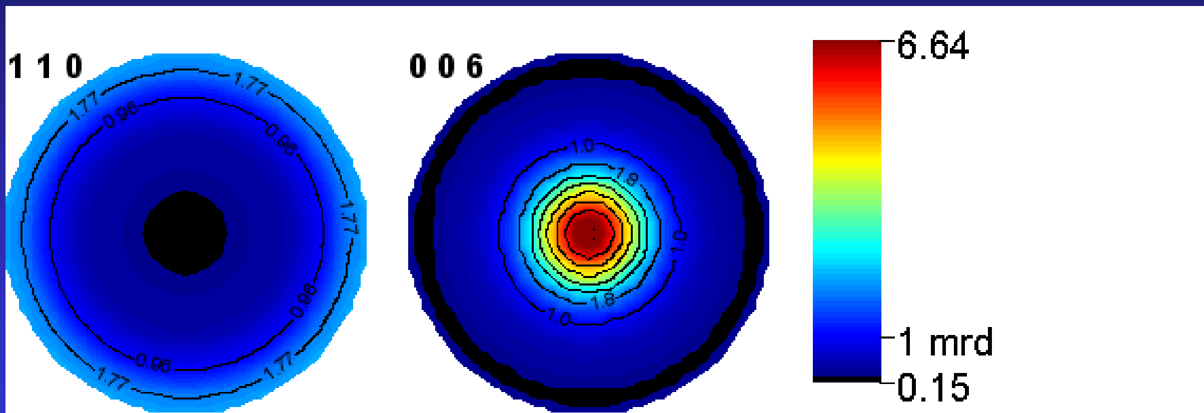

R_W (%) = 9.23
R_B (%) = 7.40

a = 4.75611(6) Å
c = 12.9806(1) Å

z_{Al} = 0.35266(3) Å
x_O = 0.6923(2) Å

Cyclic-fibre texture assumed

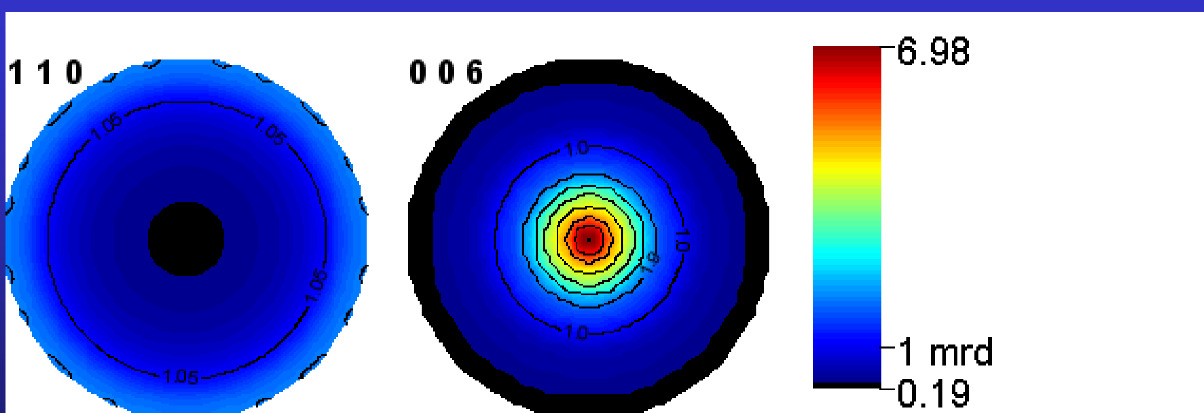

R_W (%) = 7.14
R_B (%) = 5.64

a = 4.75874(3) Å
c = 12.99373(7) Å

z_{Al} = 0.35225(2) Å
x_O = 0.6943(2) Å

ZnSe:Cr^{2+} films
N. Vivet, PhD

conditions:

- $20 \leq T_d \leq 385°C$
- P_{RF} = 50-200W
- P_{Ar} = 0.5 Pa and 2 Pa
- d = 7 and 10 cm

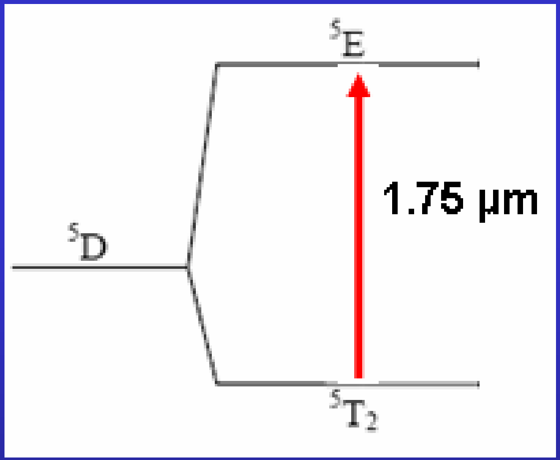

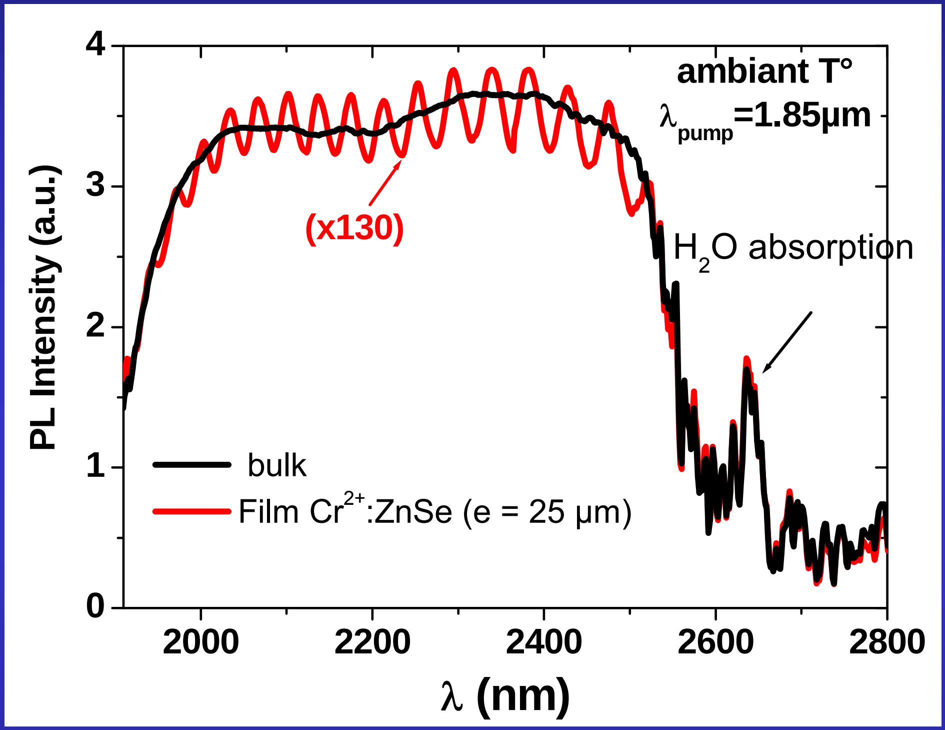

- **Large emission band centred at 2200nm: $^5E \rightarrow {}^5T_2$ transition (Cr^{2+})**
- **Single crystals and thin films: similar spectra**

111 Peak shifts

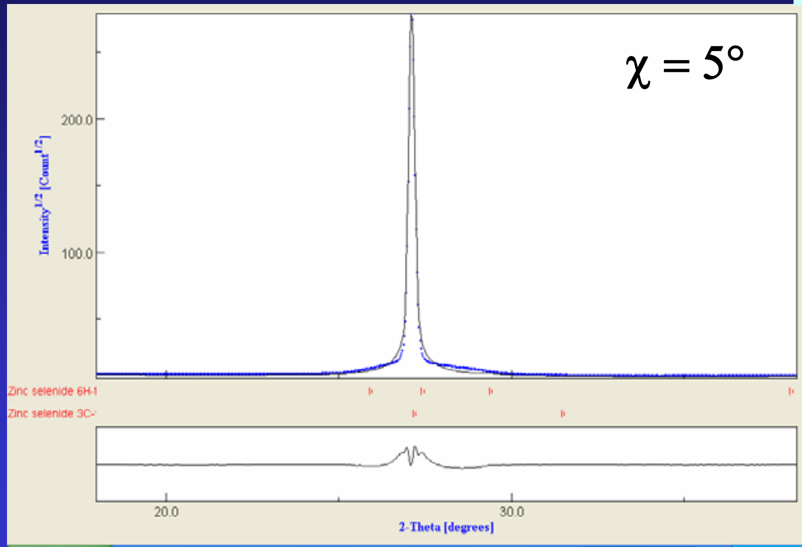

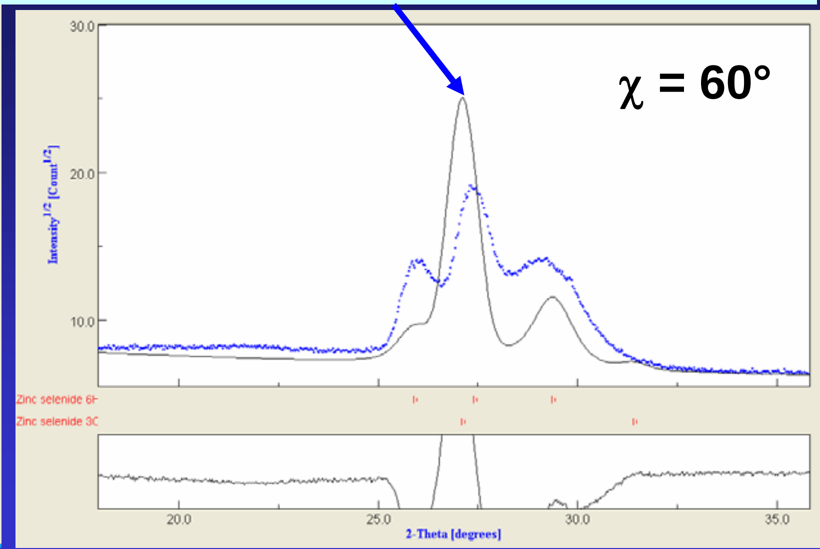

Residual stresses and/or stacking faults

Anisotropic sizes

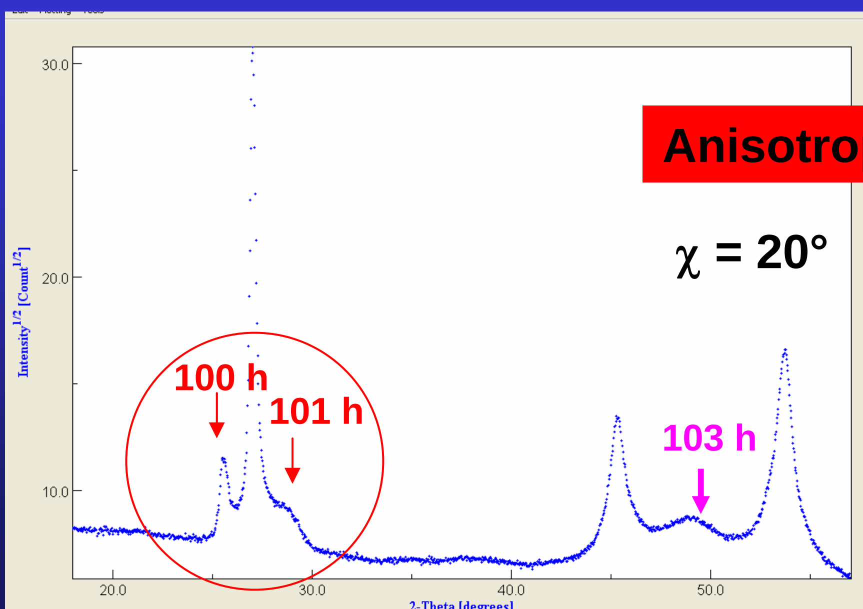

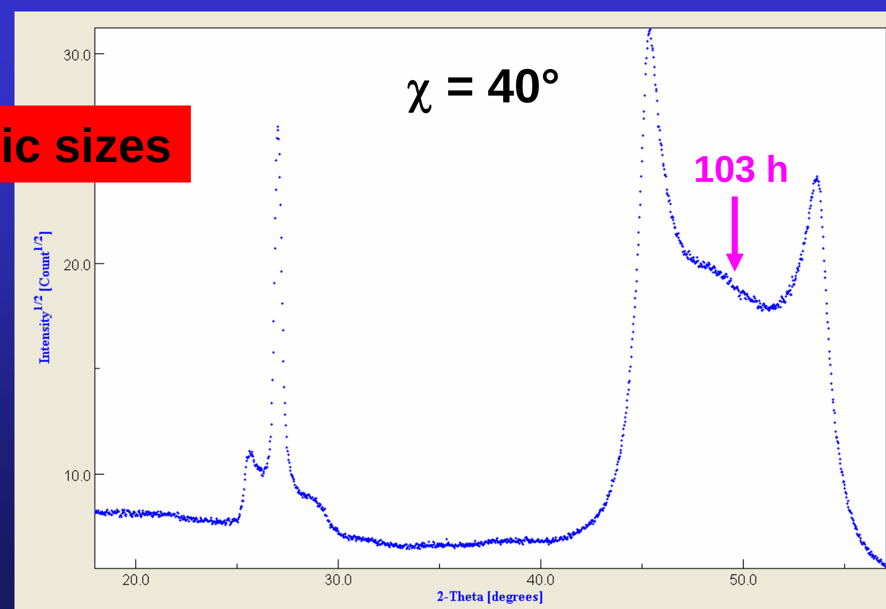

Fibre Texture + 2 polytypes (6H and 3C) + anisotropic sizes + residual stresses and/or stacking faults + layering

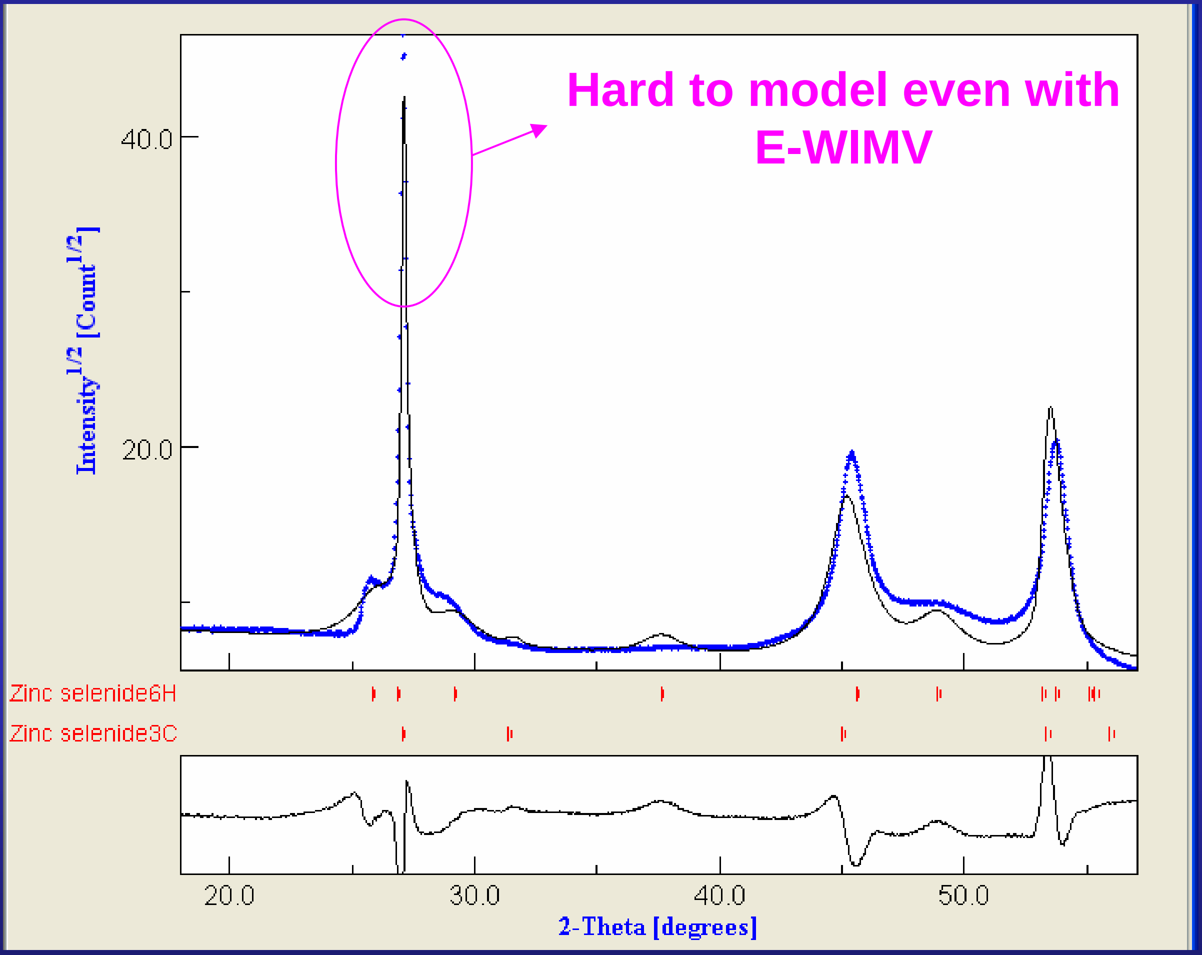

Sum diagram: ω =13.65°, P_{RF} = 200W

Independent measurements

Different wavelengths and rays

Reflectivity: thickness, roughness, electron density profiles

X-ray Fluorescence: composition

Spectroscopies: local structures (PDF, FTIR, Mossbauer …), eventually anisotropic (P-EXAFS, ESR, Raman …), Element profiles (SIMS, RBS …) …

Physical models: magnetisation, conductivity …

Specular reflectivity: **q**=(0,0,z)

- Fresnel:

$$R(\mathbf{q}) = \left| \frac{q_z - \sqrt{q_z^2 - q_c^2 + \frac{32i\pi^2\beta}{\lambda^2}}}{q_z + \sqrt{q_z^2 - q_c^2 + \frac{32i\pi^2\beta}{\lambda^2}}} \right|^2 \delta q_x \delta q$$

- matrix:

$$R^{flat} = \frac{r_{0,1}^2 + r_{1,2}^2 + 2r_{0,1}r_{1,2}\cos 2k_{Z,1}h}{1 + r_{0,1}^2 r_{1,2}^2 + 2r_{0,1}r_{1,2}\cos 2k_{Z,1}h}$$

- Born approximation:
  Electron Density Profile

$$R(q_z) = r.r^* = R_F(q_z)\left| \frac{1}{\rho_s} \int_{-\infty}^{+\infty} \frac{d\rho(z)}{dz} e^{iq_z z} dz \right|^2$$

- Roughness:

$$R^{rough}(q_z) = R(q_z)\exp(-q_{z,0}q_{z,1}\sigma^2) \quad \text{Low-angles (reflectivity)}$$

$$S_R = 1 - p\exp(-q) + \mathrm{p}\exp\left(\frac{\text{-q}}{\sin\theta}\right) \quad \text{high-angle (Suortti)}$$

CPS scans

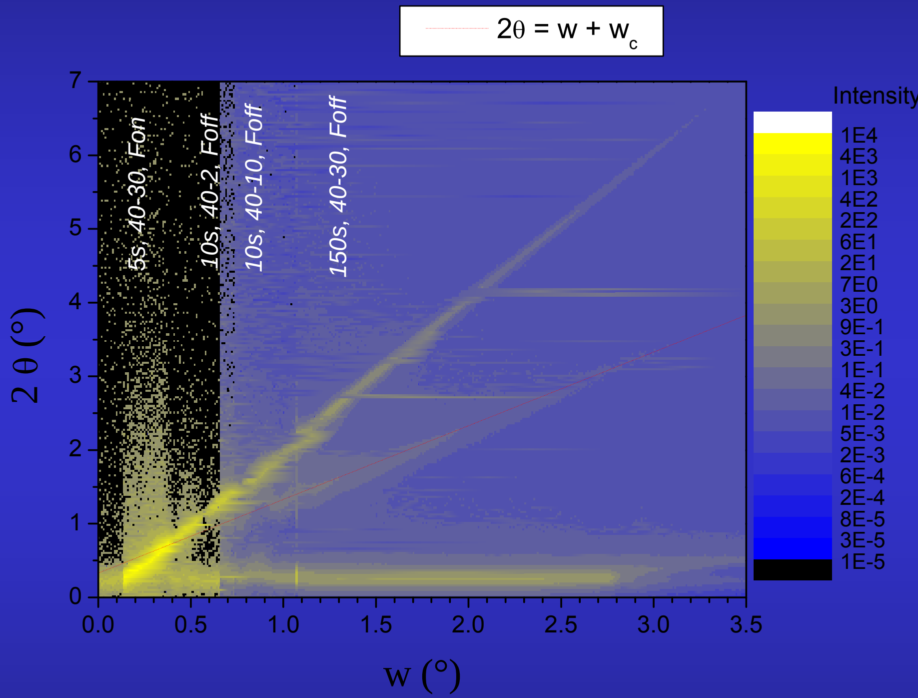

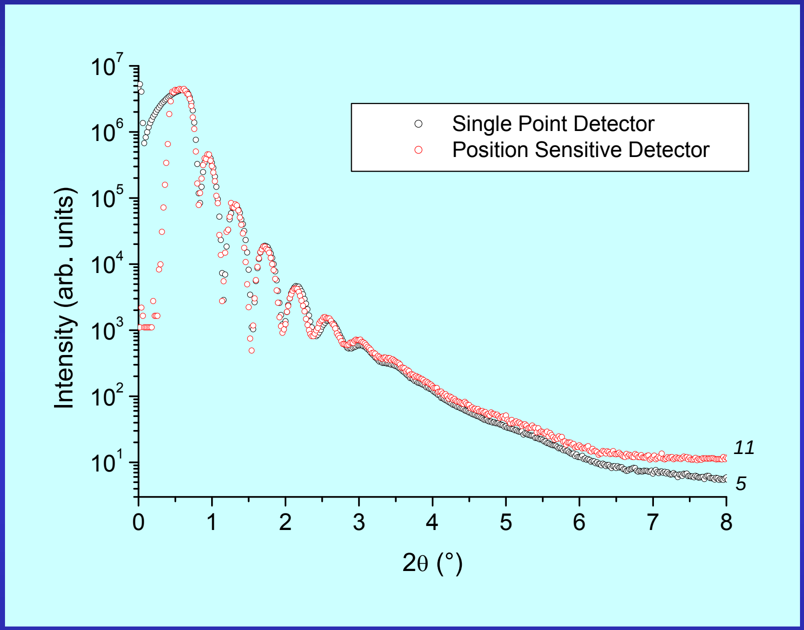

Useful for having bot specular and off-specular signals in one scan

Conclusions

a) Texture affects phase ratio and structure determination

b) Microstructure (crystallite size) affects texture (go to a)

c) Stresses shift peaks then affects structure and texture determination

d) Combined analysis may be a solution, unless you can destroy your sample or are not interested in macroscopic anisotropy ...

e) If you think you can destroy it, perhaps think twice

f) more information is always needed: local probes ...

g) Combined Analysis (D. Chateigner Ed), Wiley-ISTE 2010